3.A:2.B

Nuclear Physics **A173** (1971) 146—176; © *North-Holland Publishing Co., Amsterdam*

STRUCTURE OF ^{61}Cu VIA ^{58}Ni(^{4}He, pγ) HIGH-RESOLUTION PROMPT p-γ COINCIDENCE SPECTROMETRY

E. J. HOFFMAN †, D. G. SARANTITES and N.-H. LU

Department of Chemistry, Washington University, St. Louis, Missouri 63130, USA ††

Received 9 March 1971
(Revised 19th May 1971)

Abstract: The level structure and the detailed decay properties of the levels in ^{61}Cu have been studied via prompt γ-ray energy and intensity measurements utilizing a NaI(Tl)-Ge(Li) anti-Compton spectrometer and pγ prompt coincidence techniques via the ^{58}Ni(^{4}He, pγ)^{61}Cu reaction with ^{4}He^{++} energies in the range 4.6–12.5 MeV. Many of the γ-rays associated with levels in ^{61}Cu were identified with the (^{4}He, pγ) reaction by means of extensive on-beam pγ coincidence measurements employing a 41 cm^3 Ge(Li) γ-ray detector and several annular Si(Li) or surface-barrier charged-particle detectors. Characterization of many levels in ^{61}Cu was aided considerably by a high-resolution study of the proton spectrum from the ^{58}Ni(^{4}He, p) reaction employing a tandem Van de Graaf accelerator and a split-pole Enge magnetic spectrograph. It was thus established that 50 levels up to 4.0 MeV in excitation are populated by this reaction in ^{61}Cu and that these accommodate 98 γ-rays. Branching ratios for the γ-de-excitation of 48 levels in ^{61}Cu were obtained by averaging the measured angular correlation of each γ-ray about the beam direction. The directional correlation of 18 primary γ-rays in coincidence with protons detected at approximately 180° with respect to the beam direction were measured and the results were used to assign definite J-values for many levels in ^{61}Cu. A detailed level scheme for the de-excitation of levels in ^{61}Cu is offered.

E

NUCLEAR REACTIONS ^{58}Ni(^{4}He, pγ), E = 4.6–12.5 MeV; measured E_p, E_γ, I_γ, $I_\gamma(\theta)$, pγ coinc., p$\gamma(\theta)$. ^{61}Cu deduced levels, J, π, δ, γ-branching. Enriched targets, magnetic spectrograph, Ge(Li), NaI(Tl)-Ge(Li) anti-Compton spectrometers, Si(Li) and Si surface-barrier annular detectors, $E \cdot \Delta E$ Si(Li) telescope.

1. Introduction

The levels in ^{61}Cu have been investigated recently [1, 2]) by means of high-resolution techniques from the decay of 86 sec ^{61}Zn. The levels in ^{61}Cu have also been recently investigated by a variety of nuclear reactions such as (p, $\gamma\gamma$), (^{3}He, d), (p, α) and (d, n) and the pertinent references were given by Hoffman and Sarantites [2]).

The present study is an attempt to obtain a detailed characterization of the low-lying level structure of ^{61}Cu, which is considered essential for reliable interpretation of the results of a study of the mechanism of the nuclear reactions induced by ^{4}He^{++} on ^{58}Ni (see the following paper). During the preparation of this manuscript Heusch

† Present address: Bartol Research Foundation, Swarthmore, Pennsylvania.

†† This work was supported in part by the US Atomic Energy Commission under contract No. At(11-1)-1530 and At(11-1)-1760.

et al. [3]) reported results of some pγ correlation work in ^{58}Ni(^{4}He, pγ) for levels up to 1942 keV. Their J^{π} assignments are in good agreement with the results of this work, but minor differences exist in the reported multipole mixing ratios. In the present study we have extended the assignment of γ-rays and J^{π} values to levels in ^{61}Cu for excitation energies up to 4.0 MeV and have made more definite J^{π} assignments for some of the lower lying levels in ^{61}Cu.

2. Experimental procedures

2.1. THE CYCLOTRON FACILITY

The external beam facility of the Washington University cyclotron was used to provide the 4.6–12.5 MeV ^{4}He ion beams required. This facility has been described in some detail elsewhere [4]). The lowest energy $^{4}He^{++}$ beam that is conveniently available at present at the Washington University cyclotron is 12.5 MeV. Experiments at lower bombardment energies were performed by degrading the beam energy by means of Ta or Au foils. Extensive singles measurements with the attenuated beam were performed only at 8.6 MeV of average bombardment $^{4}He^{++}$ energy. In all the pγ coincidence experiments the unattenuated beam of 12.5 MeV $^{4}He^{++}$ was employed. The beam currents used varied between 2–150 nA.

2.2. SCATTERING CHAMBERS AND CHARGED-PARTICLE COUNTING

Three different target mounting assemblies were used in this work and are briefly described below.

2.2.1. *A miniature scattering chamber.* For the singles measurements, the singles angular correlations and the pγ coincidence angular correlations a miniature scattering chamber was used (outer diameter 7.8 cm). An annular Si(Li) detector or a Si surface-barrier detector which had an active area of 300 mm^2 and 1.0 mm depletion depth with a 4 mm diameter hole were employed in this work. These detectors were mounted on a copper cold finger and were operated at −77°C to reduce noise. The detector to target distance varied between 15.0 and 25.0 mm. A 50 mm^2 Si surface-barrier detector was positioned at 90° with respect to the beam direction and it was used as a monitor of the elastically scattered particles in the singles correlations. The scattering chamber was lined with 200 mg/cm^2 Ta foil sufficient to stop 30 MeV $^{4}He^{++}$, in order to avoid γ-ray producing reactions in the Al material of the chamber. A 1.6 mm inner diameter and 2.0 mm outer diameter Ta collimator was also used to guide the beam to a point past the annular Si detector. For the majority of the measurements the Ta X-rays which are produced with substantial intensity were absorbed by using 0.5 mm Cd absorber in front of the Ge(Li) detector. Other γ-rays from Coulomb excitation in Ta did not interfere since they are produced only with low intensity.

2.2.2. *A precision* 110 cm *scattering chamber.* In order to measure the singles proton and α-particle spectra from the (^{4}He, p) and (^{4}He, α′) reactions a ($E \cdot \Delta E$) mass identifying telescope was used. This consisted of a 1.0 mm × 1.0 cm^2 Si(Li) detector for the total absorption detector and a 0.100 mm × 1.0 cm^2 totally depleted Si(Li) detector. This detector assembly was cooled to −40°C with a thermoelectric cooler, and it was mounted in a precision 110 cm diameter scattering chamber on a detector supporting arm that could be remotely positioned at the required angle [5]). A linear adder (Argonne Model M-133) was used to linearly add the ΔE and E' signals and the resulting total energy pulse was fed with the ΔE pulse to a pulse multiplier. The resulting mass spectrum indicated that for the energies used in this work only protons and α-particles were emitted in detectable amounts.

2.2.3. *A large solid-angle assembly.* For measurements of pγ coincidence spectra a target mounting assembly which provided the maximum solid angle for both the Si(Li) and Ge(Li) detectors was employed. This consisted of a narrower beam tube (4.0 cm in diameter) which held the target at a distance of 1.9 cm from the annular detector. In this arrangement the Ge(Li) detector was placed at 90° to the beam direction at an actual distance from the target of 2.5 cm. Here the beam was stopped in a Pb dump 2 m away from the detectors.

2.3. GAMMA-RAY COUNTING

For γ-ray counting a 29 cm^3 Ge(Li) detector with a typical resolution of 2.8 keV (FWHM) for the 1332 keV line of ^{60}Co was employed in an anti-Compton arrangement. The anti-coincidence detector was an annular NaI(Tl) scintillation crystal with a 19 cm diameter and 12.7 cm length. The performance characteristics and the calibration of this spectrometer have been described in some detail in ref. [6]). This spectrometer and its lead shield were mounted on an angular correlation table. For precision γ-ray energy measurements the spectrometer was placed at 90° with respect to the beam to minimize distortion of the γ-peaks due to Doppler shift and broadening.

At ^{4}He^{++} bombardment energies higher than 10.1 MeV, ^{61}Zn is produced by the reaction ^{58}Ni(^{4}He, n). This results in a background of "delayed" γ-rays which are common with many prompt ones. Additional delayed background is contributed by the radioactivity of the 3.3 h ^{61}Cu which grows in the target with time. In order to identify and measure the intensity of the delayed γ-rays several pulsed experiments were performed. In these measurements the low-level power supply of the r.f. oscillator of the cyclotron was turned on and off with the aid of a preset interval timer through a double mercury relay switch. The pulses from the Ge(Li) detector system were routed to the second half of the 4096-channel pulse-height analyser when the r.f. was off and to the first half when it was on. The spectra were accumulated by repeating a cycle of a counting interval of 200 ms with the beam on, followed by 200 ms with the beam off.

For the pγ coincidence experiments a 40.8 cm^3 Ge(Li) detector with an active area

of 10.7 cm^2 and length of 3.80 cm was employed. This detector had a typical resolution of 2.3 keV and a peak-to-Compton ratio of 25 : 1 for the 1332 keV line of ^{60}Co. This detector was also mounted on another angular correlation table and could be rotated between 0°–90° with respect to the beam and outside the miniature scattering chamber. This arrangement was employed in the pγ coincidence correlation experiments.

For the energies employed in this work the period between beam bursts from the cyclotron was 140 ns while the width of each burst was $\approx$ 4 ns. Since in the present experiments the most prominent reaction was (^{4}He, pγ), it was possible to operate at low beam currents so that, on the average, no more than one γ-ray producing event occurred per ten beam bursts. Under these conditions pγ coincidence events could be accumulated at a rate as high as 100 c/sec with random coincidence events not exceeding the limit of $\approx$ 8 % of the total coincidence rate. It should be noted that the prompt coincidence peak had a width at 1/10 height of $\approx$ 70 ns for γ-ray pulses in the energy range of 80–2600 keV and for proton pulses in the range of 2.0–10.0 MeV. This timing resolution was sufficient to completely reject contribution to the random rate from the neighboring satellite beam bursts.

For pulse-height analysis a Nuclear Data, Inc., Model No. 161 4096-channel two-parameter pulse-height analyzer was used. The analyzer was equipped with a buffer tape and a read-search control unit, coupled with an IBM computer compatible magnetic tape drive. This analyzer with 18-bit related address capability was employed in all the pγ coincidence and correlation experiments.

2.4. HIGH-RESOLUTION PROTON SPECTROSCOPY

High-resolution proton spectra from the ^{58}Ni(^{4}He, p) reaction were obtained using the tandem Van de Graaff accelerator at Argonne National Laboratory in conjunction with an Enge split-pole magnetic spectrograph. The design and operational characteristics of the spectrograph have been described in ref. [7]). In order to eliminate any α-particle tracks cellulose triacetate absorber sufficient to stop the α-particles but not the protons was placed in front of the emulsion plates. The number and position of all the tracks were determined with an automatic nuclear emulsion scanner, which was coupled to a PDP-9 digital computer programmed to control the scanning head and to do pattern recognition. A high-resolution image-dissection tube scanned the emulsion plates with a resolution width of about 5 μm. The scanner made 10 μm sweeps on the plate and then integrated the number of tracks for every 0.5 mm.

2.5. PREPARATION OF THE TARGETS

The targets employed in the pγ coincidence work were self-supporting foils (480 μg/cm^2) of nickel metal enriched to 99.89 % in mass 58 with 0.11 % contamination from mass 60. These foils were prepared by rolling of the metal.

The targets employed in the high-resolution proton work consisted of $\approx$ 50 μg/cm^2 ^{58}Ni deposits on 50 μg/cm^2 carbon backing and were prepared with the use of an isotope separator at the Argonne National Laboratory.

3. Experimental results

3.1. HIGH-RESOLUTION PROTON SPECTRA

The determination of the levels in ^{61}Cu by means of high-resolution proton spectroscopy was found very valuable in the assignment of many weak γ-ray transitions. High-resolution proton spectra from the ^{58}Ni(^{4}He, p) reaction at 12.5 MeV were

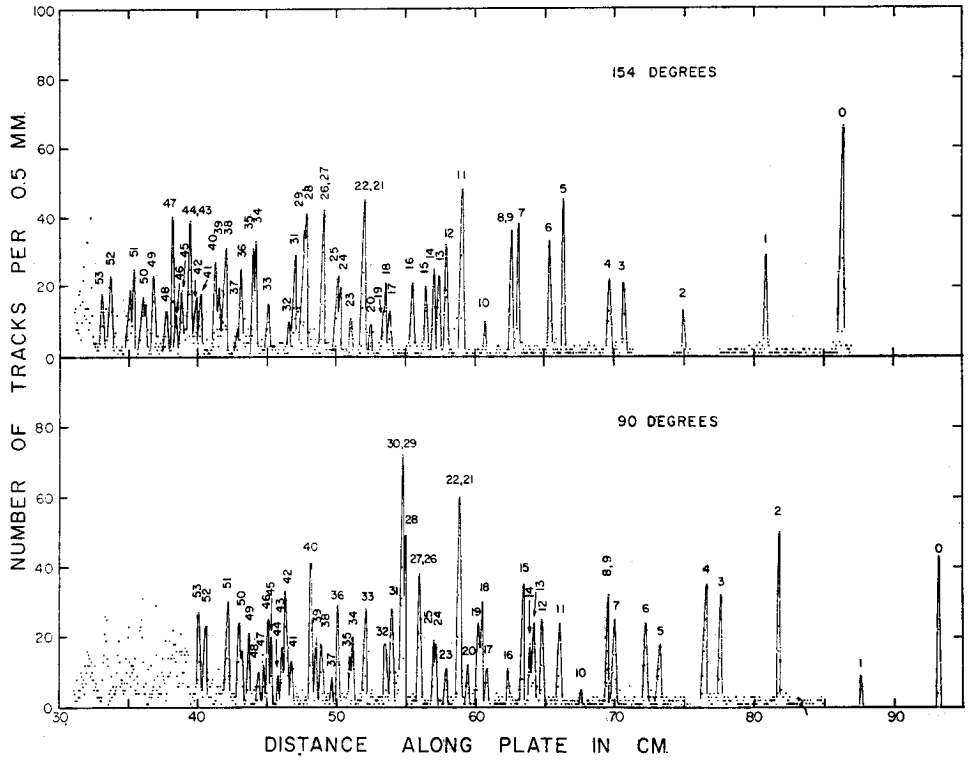

Fig. 1. High-resolution proton spectra from the ^{58}Ni(^{4}He, p) reaction at 12.50 MeV recorded with a split-pole magnetic spectrograph for the angles of 90° and 154°. The energies of the numbered proton groups are listed in table 1.

recorded with the spectrograph at two laboratory angles of 154° and 90°. The measurement at two angles served to identify proton peaks due to contaminants of different mass which exhibit different kinematic shifts. The proton spectra obtained are shown in fig. 1 and had an average resolution of 12 keV (FWHM). The proton peaks have been numbered to correspond to the levels in ^{61}Cu with the energies given in table 1. From this work 53 proton groups were assigned. Evidence, however, for the indicated unresolved doublets was obtained originally from the γ-ray work.

TABLE 1

Energy and Q-value for the levels in ^{61}Cu populated in the ^{58}Ni(^{4}He, p) reaction

Level no.	Q-value [a] (MeV)	Level energy [b] (keV)	Level no.	Q-value [a] (MeV)	Level energy [b] (keV)
0	3.152 5	0	28	6.157	3005 5
1	3.631	479 2	29, 30	6.164	3012 5
2	4.122	970 2	31	6.218	3066 5
3	4.464	1312 2	32	6.247	3095 5
4	4.547	1395 2	33	6.355	3203 5
5	4.810	1658 2	34	6.412	3260 5
6	4.884	1732 3	35	6.428	3276 5
7	5.061	1919 3	36	6.484	3332 6
8, 9	5.090	1938 3	37	6.516	3364 6
10	5.240	2088 3	38	6.558	3406 6
11	5.359	2207 3	39	6.589	3437 6
12	5.446	2294 3	40	6.611	3459 6
13	5.487	2335 3	41	6.680	3528 6
14	5.512	2360 3	42	6.704	3552 6
15	5.552	2400 3	43	6.730	3578 6
16	5.624	2472 3	44	6.749	3597 6
17	5.738	2586 4	45	6.770	3618 6
18	5.762	2610 4	46	6.798	3646 6
19	5.780	2628 4	47	6.812	3660 6
20	5.836	2684 4	48	6.838	3686 7
21, 22	5.874	2722 4	49	6.900	3748 7
23	5.945	2793 4	50	6.954	3802 7
24	5.995	2843 4	51	6.996	3844 7
25	6.011	2859 4	52	7.095	3943 7
26, 27	6.078	2926 4	53	7.130	3978 7

[a]) The standard deviation was estimated to be 8 keV. The Q-value for the ground state was obtained as a weighted average of the value resulting from the Q-values of the first 20 single levels using the level energies established in the γ-ray work.

[b]) The standard deviation for the level energies was estimated by comparison with the values obtained from the more accurate γ-ray work.

3.2. ENERGIES OF THE PROMPT γ-RAYS FROM ^{58}Ni(^{4}He, pγ)^{61}Cu

The energies of the prompt γ-rays from the ^{58}Ni(^{4}He, pγ) reaction were measured for a series of bombardment energies covering the range 4.6–12.5 MeV. For energy determinations the Compton-suppression spectrometer was used at 90° to the beam direction. Accurate γ-ray energies were determined utilizing as internal standards (i) the γ-rays in ^{61}Cu for which accurate values were obtained [2]) from the study of the decay of ^{61}Zn, and (ii) the γ-rays from the decay [9]) of the 3.3 h ^{61}Cu. In figs. 2 and 3 we show representative Compton-suppressed spectra of the γ-rays from the ^{58}Ni(^{4}He, pγ) reaction at 5.8 and 10.0 MeV. In fig. 3 the "delayed" and extraneous γ-rays are properly labelled. The "delayed" spectrum in fig. 3 is due to γ-rays from ^{61}Cu decay and is displayed by the lower spectrum. The various sources of γ-rays extraneous to the target were determined, in a number of preliminary experiments.

First, for bombardment energies near and below 10.1 MeV [the (^{4}He, n) threshold] no substantial background was observed without the target. When the beam energy is reduced to 5.6 MeV the (^{4}He, p) cross section decreases drastically to the extent that some background γ-rays become noticeable. These background γ-rays are due to reactions induced by a small number of neutrons produced from impurities on the beam slits and collimators. These neutrons were found to produce interfering γ-rays

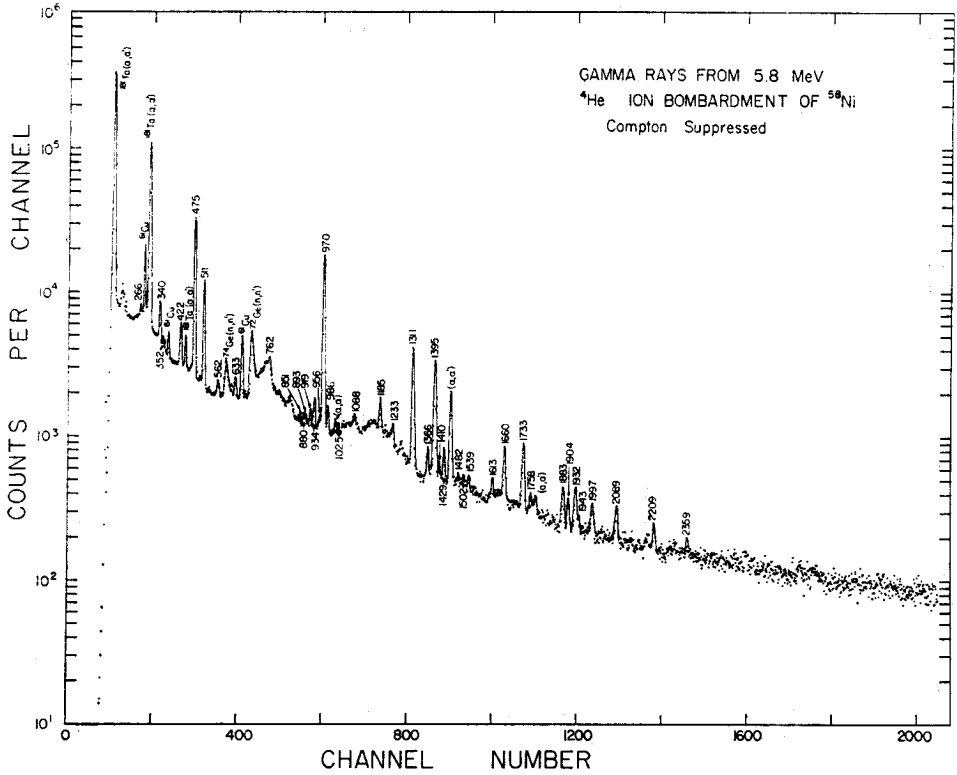

Fig. 2. Compton-suppressed spectrum of the prompt γ-rays from the ^{58}Ni(^{4}He, pγ) reaction at 5.8 MeV. The γ-rays following ^{61}Cu decay are labeled (^{61}Cu), γ-rays from inelastic ^{4}He scattering in the target are indicated as (α, α') and in ^{181}Ta as ^{181}Ta(α, α') and γ-peaks from inelastic neutron excitation in the Ge of the detector are indicated as Ge(n, n').

primarily from (n, n'γ) reaction in the Ge isotopes of the detector, in ^{23}Na and ^{127}I of the NaI(Tl) annulus and to a much smaller extent from (n, γ) induced radioactivity. For bombardments at 12.5 MeV small amounts of 86 sec ^{61}Zn activity are produced. The background radiations at this energy do not produce observable γ-peaks in the spectrum since the cross section for the (^{4}He, p) reaction is much larger than that of the extraneous processes. In table 2 we summarize the γ-rays associated with the decay of levels in ^{61}Cu assigned in this work. The first, third and fifth columns give the transition between levels as numbered in this work, and the second, fourth and sixth columns give the measured γ-ray energies from this work.

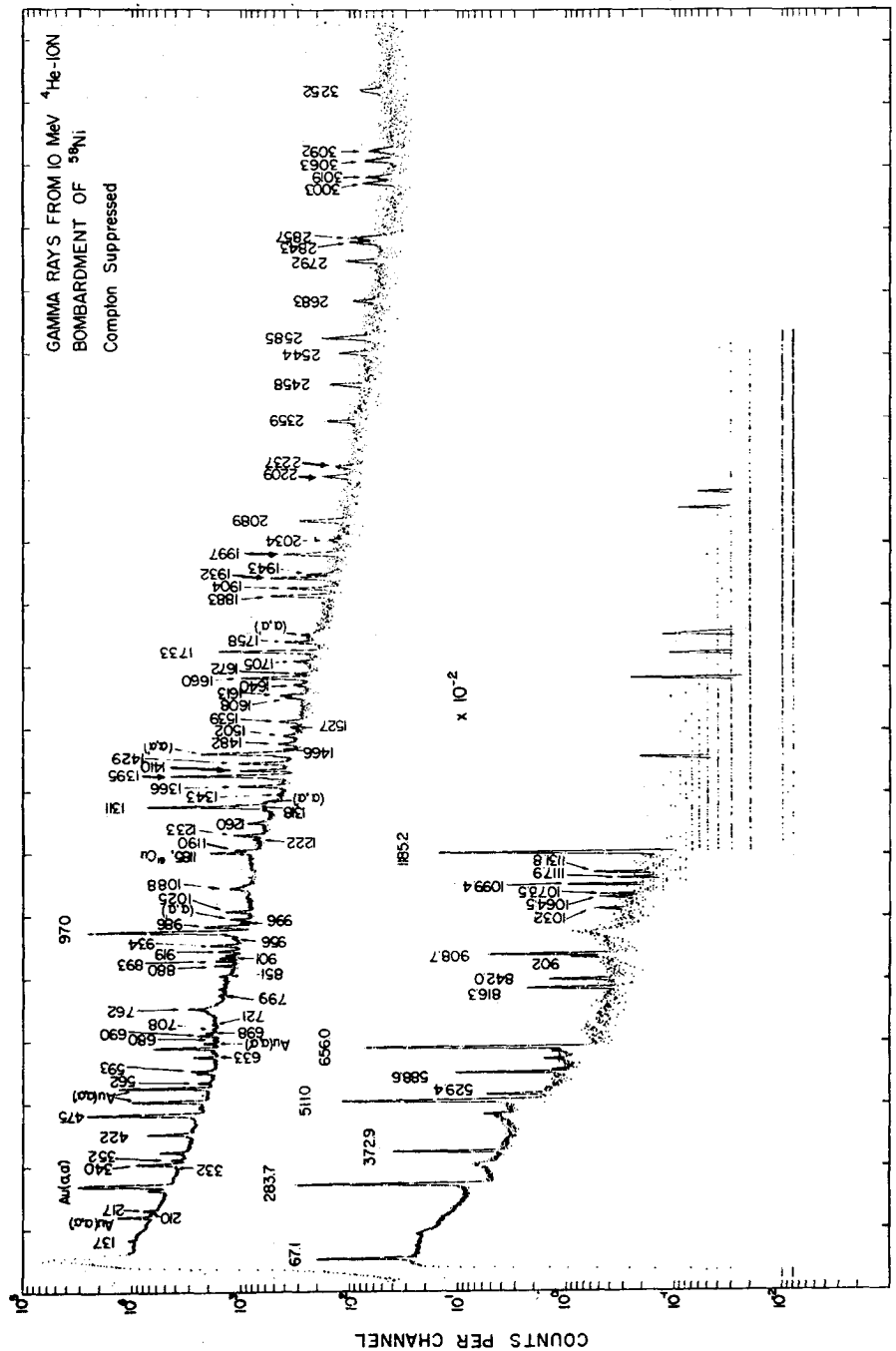

Fig. 3. Compton-suppressed spectrum of the prompt γ-rays from ^{58}Ni(^{4}He, pγ) at 10.0 MeV. The contaminant γ-rays are labeled in the upper spectrum using the notation of fig. 2. The lower spectrum shows the "delayed" γ-rays which in this case are due to the 3.3 h ^{61}Cu decay. Here the beam degrading foil used was Au.

TABLE 2

Summary of the γ-rays associated with decay of levels in ^{61}Cu assigned in this work

Transition	γ-ray energy (keV)		Transition	γ-ray energy (keV)		Transition	γ-ray energy (keV)	
9 → 6	209.7	2	41 → 19	955.5	3	31 → 4	1672.0	6
19 → 13	229.6	13	2 → 0	970.3	2	29 → 3	1705.3	3
5 → 4	265.9	1	9 → 2	972.4	6	6 → 0	1732.6	1
19 → 12	332.3	10	12 → 3	985.6	2	22 → 2	1758.1	2
3 → 2	340.0	3	13 → 3	1025.2	10	14 → 1	1883.1	3
12 → 9	352.1	3	35 → 15	1074	2	7 → 0	1904.1	9
6 → 3	421.7	4	15 → 3	1088.4	4	8 → 0	1932.4	1
4 → 3	424.2	10	48 → 21	1131.5	7	9 → 0	1943.0	3
14 → 10	426.0	4	5 → 1	1185.3	3	16 → 1	1997.4	2
1 → 0	475.0	1	26 → 6	1190.3	4	36 → 3	2012.8	9
2 → 1	494.9	2	49 → 22	1221.6	4	10 → 0	2088.9	1
38 → 26	529.1	2	11 → 2	1232.8	2	38 → 3	2142.1	38
12 → 6	562.5	2	20 → 4	1289.8	6	20 → 1	2209.0	2
7 → 3	593.5	2	3 → 0	1311.0	1	41 → 2	2273	2
9 → 3	631.8	1	19 → 3	1317.9	10	43 → 3	2302	2
35 → 19	648	2	40 → 11	1342.7	4	14 → 0	2358.6	3
18 → 9	669.3	1	13 → 2	1366.2	3	25 → 1	2381.4	20
29 → 13	679.5	4	4 → 0	1394.6	1	47 → 4	2406	2
5 → 2	690.3	1	21 → 3	1409.6	4	27 → 1	2457.6	4
14 → 5	697.6	1	15 → 2	1428.9	3	30 → 1	2543.9	30
47 → 32	708.0	7	44 → 11	1444	2	17 → 0	2584.9	8
29 → 12	720.7	3	8 → 1	1457.8	1	42 → 2	2621	2
24 → 10	751.6	1	33 → 6	1465.6	2	20 → 0	2683.8	6
6 → 2	762.0	2	23 → 3	1482.1	1	23 → 0	2792.1	3
50 → 33	790	2	45 → 11	1492	2	24 → 0	2842.8	6
28 → 11	798.5	7	16 → 2	1502.4	1	25 → 0	2857.0	3
46 → 26	832	2	34 → 6	1527.0	5	27 → 0	2931.8	3
17 → 6	851.0	1	27 → 4	1538.9	2	28 → 0	3002.6	6
18 → 6	879.6	2	34 → 5	1599	2	30 → 0	3019.3	11
11 → 3	892.6	2	28 → 4	1608	2	31 → 0	3062.8	8
12 → 4	900.7	2	10 → 1	1613.3	2	32 → 0	3092.3	13
4 → 1	919.2	2	37 → 6	1640.5	6	42 → 1	3116	2
7 → 2	934.3	3	5 → 0	1660.4	1	39 → 0	3521.1	15

3.3. pγ COINCIDENCE EXPERIMENTS

Since particle identification for the pγ coincidence experiments was not found practical, typical spectra of the emitted charged particles at the backward angles were taken with a mass identification $E \cdot \Delta E$ detector telescope. In fig. 4 are shown typical spectra of the protons and α-particles from ^{58}Ni + ^{4}He^{++} at 12.5 MeV. These spectra were recorded simultaneously at 154° with respect to the cyclotron beam and indicate that the α-particles emitted in the backward angles at this bombardment energy present little or no interference in the coincidence measurements in which we do not distinguish between proton or α-particle pulses. In fact the γ-rays associated with the γ-decay of levels in ^{58}Ni are rather well known [10]) and could be easily identified by energy considerations.

The pγ coincidence relationships were established in two pγ coincidence experiments with the protons and γ-rays recorded in a two-parameter 256 × 1024 channel configuration for the Si(Li) × Ge(Li) detectors, respectively. In these experiments an annular Si detector and the 40.8 cm^3 Ge(Li) detector were employed. The proton energy axis covered a range of 2.0–14.0 MeV, while the Ge(Li) axis covered a range of 180–2600 keV. The γ-ray spectra recorded with the Ge(Li) detector were analysed for every 150 keV of the range of the proton axis. The pγ coincidence relationships

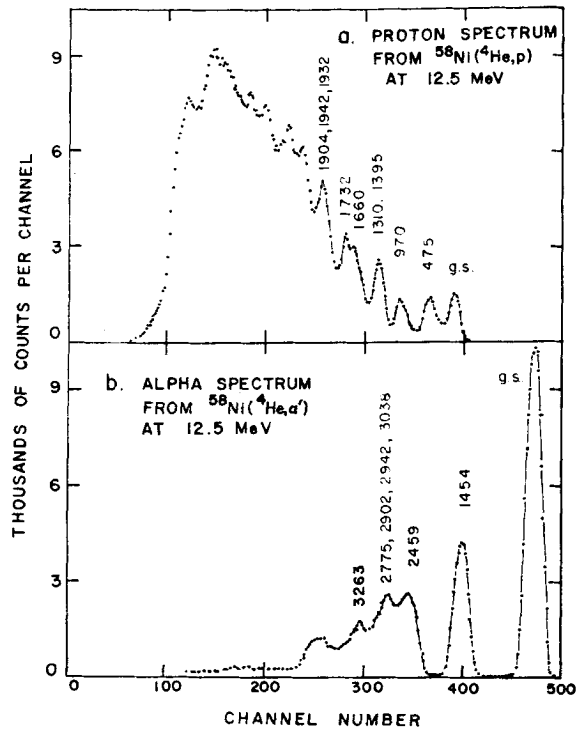

Fig. 4. Typical proton and α-particle spectra from a 12.5 MeV ^{4}He^{++} bombardment of ^{58}Ni, recorded at 154° with respect to the beam with the $E \cdot \Delta E$ detector telescope. Only major energy groups are labeled.

established in this work helped assign 98 γ-rays to the decay of 50 levels in ^{61}Cu. Figs. 5–7 illustrate some γ-ray spectra recorded with the Ge(Li) detector in coincidence with protons populating levels in ^{61}Cu which lie in the given excitation energy ranges. To minimize the number of illustrations necessary to present the coincidence information the energy range of each proton gate was increased to ≈ 300 keV. The pγ coincidence information is summarized in table 3. The last column in table 3 indicates which of the γ-rays of column 4 were observed in coincidence with the protons populating the level given in column 2.

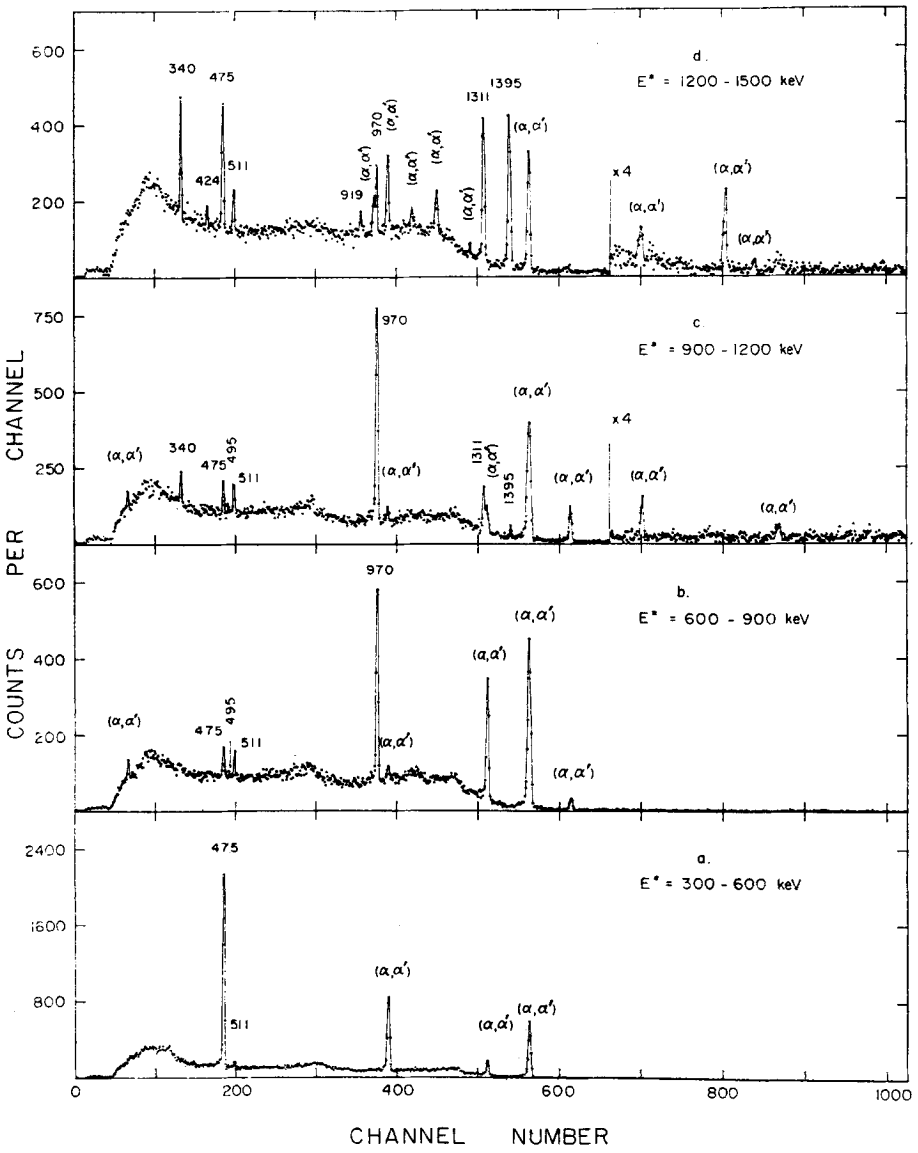

Fig. 5. Spectra of the γ-rays recorded with the 41 cm^3 Ge(Li) detector in coincidence with protons from the ^{58}Ni(^{4}He, p)^{61}Cu reaction corresponding to the indicated regions of excitation energy in ^{61}Cu.

3.4. BRANCHING RATIO EXPERIMENTS

Branching ratios for the de-excitation of 48 levels in ^{61}Cu were determined from measurements of the angular distributions of the singles γ-rays relative to the beam direction. Experiments were performed at 8.6 MeV ^{4}He^{++} bombardment energy.

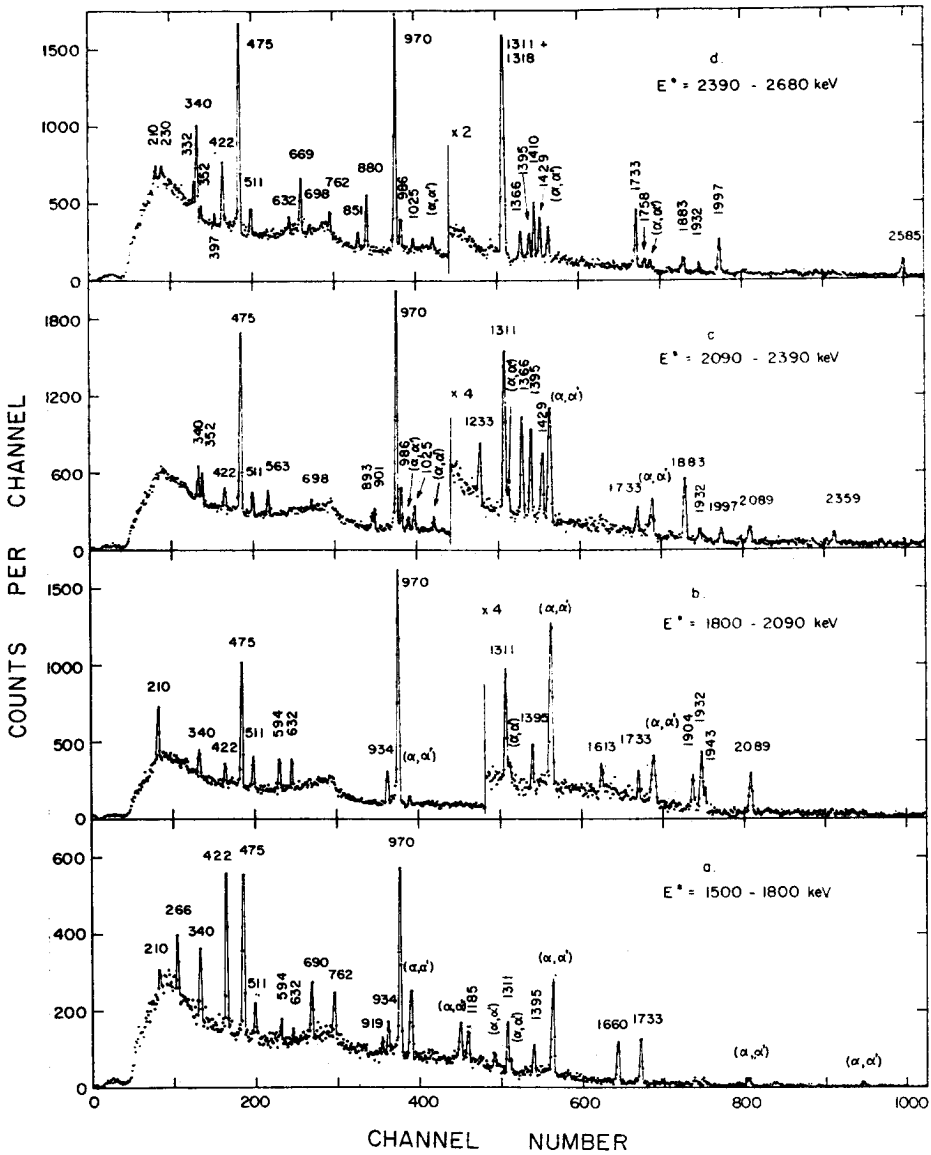

Fig. 6. Spectra of the γ-rays recorded with the 41 cm^3 Ge(Li) detector in coincidence with protons from the ^{58}Ni(^{4}He, p)^{61}Cu reaction corresponding to the indicated regions of excitation energy in ^{61}Cu.

At this energy the ^{61}Zn is not produced and prompt singles correlations could be determined without correction for contribution from radioactivity. In these experiments the beam intensity was monitored by recording the elastic (^{4}He, α') scattering events with a surface-barrier detector positioned at 90° to the beam and by means of a cur-

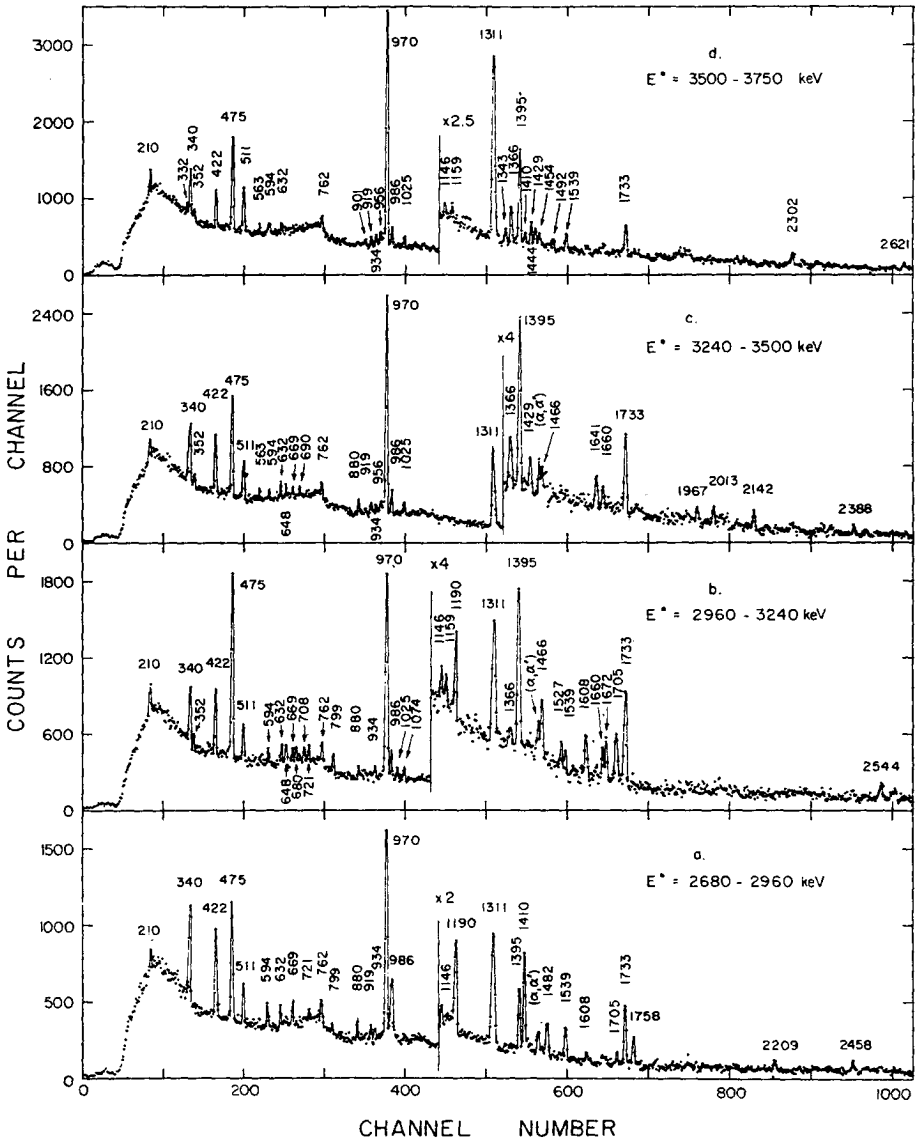

Fig. 7. Spectra of the γ-rays recorded with the 41 cm^3 Ge(Li) detector in coincidence with protons from the ^{58}Ni(^{4}He, p)^{61}Cu reaction corresponding to the indicated regions of excitation energy in ^{61}Cu.

rent integrator. The correlations for the $475(\frac{1}{2} \rightarrow \frac{3}{2})$, $970(\frac{5}{2} \rightarrow \frac{3}{2})$, $422(\frac{7}{2} \rightarrow \frac{7}{2})$ and $919(\frac{5}{2} \rightarrow \frac{1}{2})$ keV transitions obtained are illustrated as an example in fig. 8. As expected the $475(\frac{1}{2} \rightarrow \frac{3}{2})$ keV transition is isotropic, while the $919(\frac{5}{2} \rightarrow \frac{1}{2})$ keV transition shows a correlation characteristic of a quadrupole transition. The branching ratios

for many levels were determined by proper averaging of the measured distributions and the results are summarized in column 5 of table 3. In this table the first column gives the level number, the second column gives the level energy established in this work, the third column gives the J^{π} value deduced in this work (see subsect. 3.5) and the fourth column gives the γ-ray energy de-exciting the level in question. The branching ratios for the 1660.5, 2088.8, 2358.2, 2684.0, 2840.7, 2933.3 and 3019.2 keV levels

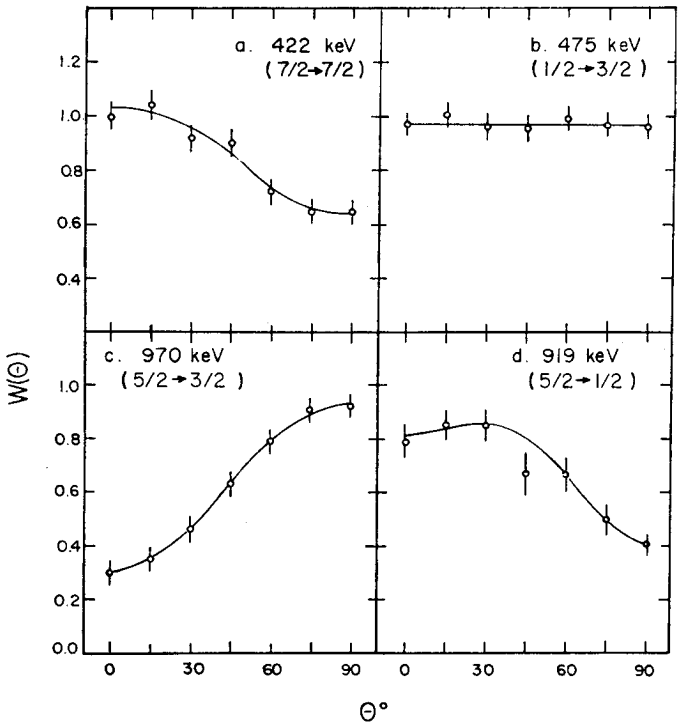

Fig. 8. Typical singles correlations of the 422, 475, 970 and 919 keV γ-rays about the beam direction. Notice that the 475 keV distribution is isotropic, while that of the 919 keV is characteristic of quadrupole transitions. The numbers in parentheses give the $J_1 \rightarrow J_2$ sequence for each transition.

were taken from ref. [2]) as these levels are more strongly populated in ^{61}Zn decay. For some of the levels above 3002.3 keV branching ratios were estimated from singles or coincidence measurements taken only at 90° to the beam where spectra with high statistics were obtained.

3.5. COINCIDENCE $p\gamma$ ANGULAR CORRELATIONS

The $p\gamma$ angular correlations for the 18 most intense transitions in ^{61}Cu were measured at 12.5 MeV $^{4}He^{++}$ bombardment energy in two two-parameter Si(Li) × Ge(Li) experiments. In this case, the Si surface-barrier detector was positioned 2.1 cm from the target, while the 41 cm^3 Ge(Li) detector was positioned at 4.1 cm from the target.

TABLE 3

Summary of level energies, J^π values, γ-ray energies and γ-ray branching ratios in ^{61}Cu determined in this work

Level no.	Level energy (keV)	J^π (this work)	γ-ray energy (keV)	Percent branching for γ-rays	γ-ray observed in pγ coincidence
0	0	$\frac{3}{2}^-$			
1	475.0 1	$\frac{1}{2}^-$	475.0 1	100	yes
2	970.3 1	$\frac{5}{2}^-$	494.9 2	0.9 1	yes
			970.3 2	99.1 6	yes
3	1311.0 1	$\frac{7}{2}^-$	340.0 3	9.4 1	yes
			1311.0 1	90.6 90	yes
4	1394.6 1	$\frac{5}{2}^-$	424.2 10	0.9 1	yes
			919.2 2	9.0 3	yes
			1394.6 1	90.1 9	yes
5	1660.5 1	$\frac{3}{2}^-$	265.9 1	4.6 3 [a]	yes
			690.3 1	15.7 12	yes
			1185.3 3	14.4 9	yes
			1660.4 1	65.3 15	yes
6	1732.6 2	$\frac{7}{2}^-$	421.7 4	28.3 2	yes
			762.0 2	7.7 4	yes
			1732.6 1	63.9 6	yes
7	1904.5 5	$(\frac{5}{2}^-)$	593.5 2	24.3 7	yes
			934.3 3	40.7 9	yes
			1904.1 9	35.0 9	yes
8	1932.5 2	$\frac{3}{2}^-$	1457.8 1	27.4 17	
			1932.4 1	72.6 43	yes
9	1942.7 2	$\frac{7}{2}^-$	209.7 2	13 2	yes
			631.8 1	24 5	yes
			972.4 6	49 10	yes
			1943.0 3	14 2	yes
10	2088.8 2	$\frac{1}{2}^-$	1613.3 2	32.1 25 [a]	yes
			2088.9 1	68 11	yes
11	2203.4 3	$(\frac{5}{2}^-)$	892.6 2	36.6 22	yes
			1232.8 2	63.4 44	yes
12	2295.4 3	$\frac{9}{2}^-$	352.1 3	7.6 4	yes
			562.5 2	17.5 5	yes
			900.7 2	21.8 10	yes
			985.6 3	53.1 12	yes
13	2336.4 10	$\frac{9}{2}^-$, $(\frac{7}{2}^+, \frac{5}{2}^+)$	1025.2 10	24.8 22	yes
			1366.2 3	75.2 10	yes
14	2358.2 2	$\frac{3}{2}^-$	426.0 4	11.1 6 [a]	yes
			697.6 1	30.7 27	yes
			1883.1 3	34.6 7	yes
			2358.6 3	23.6 17	yes
15	2399.3 5	$\frac{7}{2}^-$	1088.4 4	30.8 19	yes
			1428.9 3	69.2 34	yes
16	2472.9 2	$\frac{3}{2}^-$	1502.4 1	10.7 12	
			1997.4 2	89.3 24	yes
17	2583.7 8	$\frac{5}{2}^\pm$	851.0 1	50.4 87	yes
			2584.9 8	49.6 51	yes
18	2612.0 2	$\frac{9}{2}^-$	669.3 1	33.8 12	yes
			879.6 2	66.2 36	yes
19	2628.4 6	$(\frac{11}{2}^-, \frac{9}{2}^\pm, \frac{7}{2}^-)$	229.6 13 [b]	1.3 4 [c]	yes
			332.3 9	1.5 1	yes
			1317.9 10	97.2 93	yes
20	2684.0 4	$\frac{3}{2}^-$	1289.8 6	5.4 5 [a]	

TABLE 3 (continued)

Level no.	Level energy (keV)		J^π (this work)	γ-ray energy (keV)		Percent branching for γ-rays		γ-ray observed in pγ coincidence
				2209.0	2	52.4	29	yes
				2683.8	6	42.2	29	
21	2720.6	4	$\frac{9}{2}^+$	1409.6	4	100		yes
22	2728.4	2	$(\frac{3}{2}-\frac{7}{2})$	1758.1	2	100		yes
23	2793.0	2	$\frac{5}{2}^-$	1482.1	1	50.2	15	yes
				2792.1	3	48.8	15	
24	2840.7	3	$(\frac{1}{2}^-)$	751.6	1	55.7	70 [a]	
				2842.8	6	44.3	10	
25	2857.0	4	$(\frac{1}{2}-\frac{5}{2})^-$	2381.4	20	20	3	
				2857.0	3	80	12	
26	2922.9	4	$(\frac{3}{2}-\frac{11}{2})$	1190.3	4	100		yes
27	2933.3	3	$\frac{3}{2}^-$	1538.9	2	10.2	10 [a]	yes
				2457.6	4	78.5	46	yes
				2931.8	3	11.3	28	
28	3002.3	6	$(\frac{1}{2}-\frac{7}{2})$	798.5	7		[d]	yes
				1608	2 [b]		[d]	yes
				3002.6	6		[d]	
29	3016.1	3	$(\frac{7}{2}^-, \frac{9}{2}^\pm, \frac{11}{2}^-)$	679.5	4	16.0	33	yes
				720.7	3	16.4	34	yes
				1705.3	3	67.6	29	yes
30	3019.2	11	$(\frac{1}{2}-\frac{5}{2}^-)$	2543.9	30	71	13	yes
				3019.3	11	29	4	
31	3065.3	10	$(\frac{1}{2}-\frac{7}{2})$	1672.0	6	60	20 [e]	
				3062.8	8	40	20 [e]	
32	3092.3		$(\frac{1}{2}-\frac{5}{2})^-$	3092.3	13	100		
33	3198.2	2	$(\frac{3}{2}-\frac{11}{2})$	1465.6	2	100		yes
34	3259.6	5	$(\frac{3}{2}-\frac{7}{2})$	1527.0	5	57	20	yes
				1599	2 [b]	43	20 [c]	yes
35	3277	3	$(\frac{3}{2}-\frac{11}{2})$	648	2 [b]	67	20 [c]	yes
				1074	2 [b]	33	20 [c]	yes
36	3323.8	9	$(\frac{3}{2}-\frac{11}{2})$	2012.8	9	100		yes
37	3373.1	6	$(\frac{5}{2}-\frac{9}{2})$	1640.5	6	100		yes
38	3452	5	$(\frac{3}{2}-\frac{11}{2})$	529.1	2	28.0	14	yes
				2142.1	38	72	30 [c]	yes
39	3521.1	15	$(\frac{1}{2}-\frac{5}{2})^-$	3521.1	15	100		
40	3546.1	4	$(\frac{1}{2}-\frac{9}{2})$	1342.7	4	100		yes
41	3584.1	20	$(\frac{7}{2}^-, \frac{9}{2}^-)$	955.5	3	45	20	yes
				2273.0	20 [b]	55	20 [c]	yes
42	3591	3	$(\frac{1}{2}^-, \frac{3}{2}^\pm, \frac{5}{2}^-)$	2621	2		[d]	yes
				3116	2		[d]	yes
43	3613	2	$(\frac{3}{2}-\frac{11}{2})$	2302	2 [b]	100		yes
44	3647	2	$(\frac{1}{2}-\frac{9}{2})$	1444	2 [b]	100		yes
45	3695	2	$(\frac{1}{2}-\frac{9}{2})$	1492	2 [b]	100		yes
46	3755	2		832	2 [b]	100		yes
47	3802.0	7	$(\frac{1}{2}-\frac{9}{2})$	708.0	7	44	20	yes
				2406	2 [b]	56	20 [c]	yes
48	3852.1	7	$(\frac{5}{2}-\frac{13}{2})$	1131.5	7	100		yes
49	3950.0	4	$(\frac{1}{2}-\frac{11}{2})$	1221.6	4	100		yes
50	3988	2		790	2 [b]	100		yes

[a]) Branching fractions taken from the ^{61}Zn decay [2]).
[b]) Energy estimated from the coincidence spectra.
[c]) Intensity estimated from the coincidence spectra at 90° only.
[d]) Intensity is not given as all the γ-rays were not seen together in the same spectrum.
[e]) Intensity estimated only from singles measurements at 90°.

The Si detector subtended angles at the target between 155° and 175° with respect to the incident beam direction. In each experiment the pγ coincidence spectra were recorded for six angles for 10–12 h of counting at each angle. Since we have shown from singles correlations that the 475 keV transition to the ground state is isotropic ($J^{\pi} = \frac{1}{2}^{-}$) in these experiments we used the total coincidence 475 keV intensity at each angle as the monitor. This method of internal monitoring minimized systematic errors due

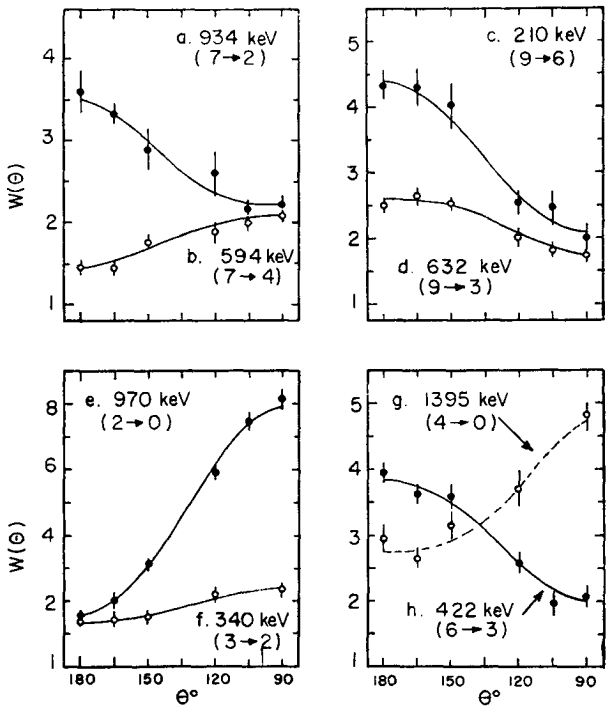

Fig. 9. The pγ correlations for the 934.3, 593.5, 209.7, 631.8, 970.3, 340.0, 1394.6 and 421.7 keV γ-transitions in ^{61}Cu. The numbers in parentheses are the level numbers that locate the transition in the ^{61}Cu decay scheme. The error bars represent only the statistical error and the solid curves are the least-squares fits of eq. (1) to the data.

to positioning of the Ge(Li) detector. Due to the limited proton resolution at this bombardment energy ($\approx$ 180 keV FWHM) only those γ-rays in coincidence with proton groups populating their originating level were considered in the analysis. Care was taken not to include in the proton gating axis contributions from higher lying levels. This was possible by digitally selecting the energy portions to be included in the proton gates. The only levels for which such interference could occur are the 1394.6, 1732.6 and 2295.4 keV levels due to the presence of the low energy 265.9, 209.7 and 332.3 keV γ-rays populating these levels, respectively. These γ-rays, however, are weak and their contribution to the selected proton gates was found negligible.

The angular correlations obtained are shown in figs. 9 and 10, where the solid lines are the least-squares fit of the data to the function

$$W(\theta) = A_0[1 + A_2 P_2(\cos\theta) + A_4 P_4(\cos\theta)]. \quad (1)$$

The analysis of the correlation data was made using the formalism and phase con-

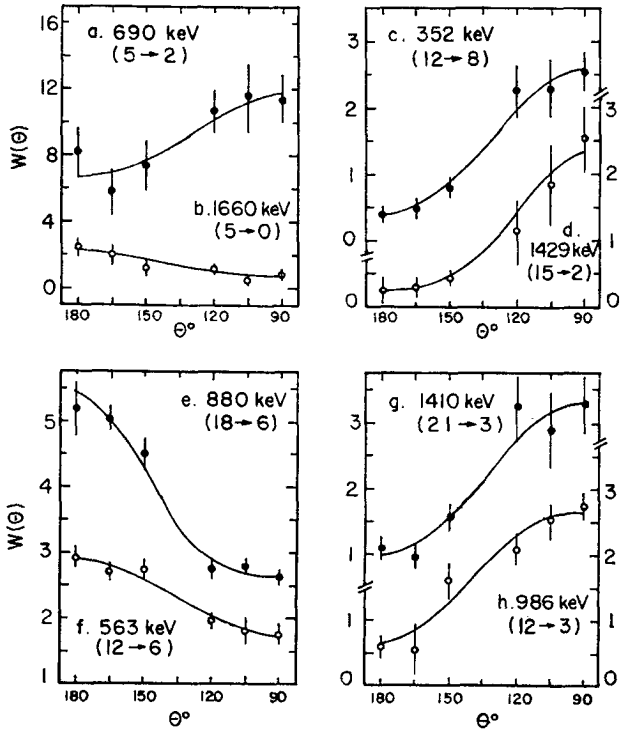

Fig. 10. The pγ correlations for the 690.3, 1660.4, 352.1, 1428.9, 879.6, 562.5, 1409.6 and 985.6 keV γ-transitions in ^{61}Cu. The numbers in parentheses are the level numbers that locate the transition in the ^{61}Cu decay scheme. The error bars represent only the statistical error and the solid curves are the least-square fits of eq. (1) to the data.

ventions of Rose and Brink [11]). The basic correlation formula is given by

$$W(\theta) = \sum_k \Big[\sum_{M_1=\frac{1}{2}}^{M_1=J_1} p(M_1)\rho_K(J_1 M_1)\Big] Q_k P_k(\cos\theta) \times \left\{\frac{R_k(LLJ_1J_2) + 2\delta R_k(LL'J_1J_2) + \delta^2 R_k(L'L'J_1J_2)}{1+\delta^2}\right\}, \quad (2)$$

which is applicable for the case of the two lowest multipoles, L and $L' = L+1$, contributing to the γ-ray transition between the initial state of total angular momentum J_1 and final state of J_2. The statistical tensors $\rho_k(J_1 M_1)$ and the coefficients R_k have been

TABLE 4

Summary of the results of the pγ angular correlations following the ^{58}Ni(^{4}He, pγ) reaction at 12.5 MeV

Transition (keV) and $J_1 \to J_2$ sequence	Experimental value [a] $R_2(J_1J_2\delta)$	$R_4(J_1J_2\delta)$	Mixing ratio δ giving solutions within 2σ
970.3 (2 → 0)			
$\frac{3}{2} \to \frac{3}{2}$	+0.99 4	0.07 3 [b]	none [d,e]
$\frac{5}{2} \to \frac{3}{2}$	+0.84 3	0.09 3	0.30 4
$\frac{7}{2} \to \frac{3}{2}$	+0.80 3	0.08 3	none [d,e]
340.0 (3 → 2)			
$\frac{3}{2} \to \frac{5}{2}$	0.44 5	0.04 7 [b]	−0.29 5 or ≦−9.0
$\frac{5}{2} \to \frac{5}{2}$	0.37 4	0.05 9	none [e]
$\frac{7}{2} \to \frac{5}{2}$	0.35 4	0.04 7	0.01 2
$\frac{9}{2} \to \frac{5}{2}$	0.35 4	0.04 7	none [d,e]
919.2 (4 → 1)			
$\frac{3}{2} \to \frac{1}{2}$	−0.71 7	0.05 10 [b]	none [d]
$\frac{5}{2} \to \frac{1}{2}$	−0.60 6	0.07 15	E2
1394.6 (4 → 0)			
$\frac{3}{2} \to \frac{3}{2}$	0.54 7	0.23 10 [b]	none [e]
$\frac{5}{2} \to \frac{3}{2}$	0.46 6	0.31 13	0.05 3 or 2.9 4
$\frac{7}{2} \to \frac{3}{2}$	0.43 6	0.25 11	none [d,e]
690.3 (5 → 2)			
$\frac{3}{2} \to \frac{5}{2}$	0.45 13	0.06 17 [b]	−0.30 14 or ≧ 4.9
$\frac{5}{2} \to \frac{5}{2}$	0.38 11	0.09 23	none [e]
$\frac{7}{2} \to \frac{5}{2}$	0.36 10	0.07 19	[f]
$\frac{9}{2} \to \frac{5}{2}$	0.35 10	0.06 17	none [d,e]
1660.4 (5 → 0)			
$\frac{3}{2} \to \frac{3}{2}$	−0.90 9	0 [c]	$-0.33 \geqq \delta \geqq -1.56$
421.7 (6 → 3)			
$\frac{3}{2} \to \frac{7}{2}$	−0.61 6	−0.07 8 [b]	none [d]
$\frac{5}{2} \to \frac{7}{2}$	−0.51 5	−0.09 11	none [e]
$\frac{7}{2} \to \frac{7}{2}$	−0.48 5	−0.07 9	$-0.24 \pm {}^{0.15}_{0.10}$
$\frac{9}{2} \to \frac{7}{2}$	−0.48 4	−0.07 8	none [e]
$\frac{11}{2} \to \frac{7}{2}$	−0.47 4	−0.06 8	none [e]
762.0 (6 → 2)			
$\frac{3}{2} \to \frac{5}{2}$	−0.60 6	−0.05 12 [b]	none [d]
$\frac{5}{2} \to \frac{5}{2}$	−0.51 5	−0.07 17	-0.12 ± 0.08
$\frac{7}{2} \to \frac{5}{2}$	−0.49 5	−0.06 15	-0.45 ± 0.08
$\frac{9}{2} \to \frac{5}{2}$	−0.48 5	−0.05 12	none [d,e]
593.5 (7 → 3)			
$\frac{3}{2} \to \frac{7}{2}$	+0.25 5	−0.07 7	none [d,e]
$\frac{5}{2} \to \frac{7}{2}$	+0.21 4	−0.09 9	0.05 ± 0.03
$\frac{7}{2} \to \frac{7}{2}$	+0.20 4	−0.07 8	0.62 ± 0.06
$\frac{9}{2} \to \frac{7}{2}$	+0.20 4	−0.07 8	-0.06 ± 0.02
$\frac{11}{2} \to \frac{7}{2}$	+0.19 4	−0.06 8	none [d,e]
934.3 (7 → 2)			
$\frac{3}{2} \to \frac{5}{2}$	−0.29 6	0.04 6 [b]	0.43 ± 0.12 or 1.38 ± 0.32
$\frac{5}{2} \to \frac{5}{2}$	−0.25 5	0.05 7	0.14 ± 0.04
$\frac{7}{2} \to \frac{5}{2}$	−0.24 5	0.04 6	-0.32 ± 0.04
$\frac{9}{2} \to \frac{5}{2}$	−0.23 5	0.04 6	none [d,e]
209.7 (9 → 6)			
$\frac{3}{2} \to \frac{7}{2}$	−0.68 7	+0.004 10 [b]	none [d]
$\frac{5}{2} \to \frac{7}{2}$	−0.57 6	+0.005 13	none [d]

TABLE 4 (continued)

Transition (keV) and $J_1 \to J_2$ sequence	Experimental value [a] $R_2(J_1J_2\delta)$	$R_4(J_1J_2\delta)$	Mixing ratio δ giving solutions within 2σ
$\frac{7}{2} \to \frac{7}{2}$	−0.55 6	+0.004 11	−0.15±0.08
$\frac{9}{2} \to \frac{7}{2}$	−0.54 6	+0.004 11	none [e]
$\frac{11}{2} \to \frac{7}{2}$	−0.53 6	+0.004 11	none [d,e]
631.8 (9 → 3)			
$\frac{3}{2} \to \frac{7}{2}$	−0.39 3	−0.11 4 [b]	none [d,e]
$\frac{5}{2} \to \frac{7}{2}$	−0.33 2	−0.12 6	none [e]
$\frac{7}{2} \to \frac{7}{2}$	−0.32 2	−0.12 5	0.26±0.06 or −0.76±0.16
$\frac{9}{2} \to \frac{7}{2}$	−0.31 2	−0.11 4	none [e]
$\frac{11}{2} \to \frac{7}{2}$	−0.30 2	−0.11 4	none [d,e]
562.5 (12 → 6)			
$\frac{3}{2} \to \frac{7}{2}$	−0.76 12	+0.11 10 [b]	none [d,e]
$\frac{5}{2} \to \frac{7}{2}$	−0.64 10	+0.15 13	none [d]
$\frac{7}{2} \to \frac{7}{2}$	−0.61 9	+0.12 11	none [e]
$\frac{9}{2} \to \frac{7}{2}$	−0.60 9	+0.11 10	−0.56±0.10
$\frac{11}{2} \to \frac{7}{2}$	−0.59 9	+0.11 10	none [d,e]
352.1 (12 → 9)			
$\frac{3}{2} \to \frac{7}{2}$	1.07 7	0.09 9 [b]	none [d,e]
$\frac{5}{2} \to \frac{7}{2}$	0.90 6	0.12 11	$-2.0 \leqq \delta \leqq -0.70$
$\frac{7}{2} \to \frac{7}{2}$	0.86 6	0.09 8	none [d,e]
$\frac{9}{2} \to \frac{7}{2}$	0.85 6	0.09 9	+0.35±0.05
$\frac{11}{2} \to \frac{7}{2}$	0.83 6	0.08 8	none [d,e]
985.6 (12 → 3)			
$\frac{3}{2} \to \frac{7}{2}$	0.69 7	0.03 6 [b]	none [d]
$\frac{5}{2} \to \frac{7}{2}$	0.58 6	0.04 8	−0.34±0.06
$\frac{7}{2} \to \frac{7}{2}$	0.56 6	0.03 6	none [d,e]
$\frac{9}{2} \to \frac{7}{2}$	0.55 6	0.03 6	0.13±0.05
$\frac{11}{2} \to \frac{7}{2}$	0.54 5	0.03 6	none [d,e]
1428.9 (15 → 2)			
$\frac{3}{2} \to \frac{5}{2}$	1.38 11	+0.44 13 [b]	none [d,e]
$\frac{5}{2} \to \frac{5}{2}$	1.18 9	0.58 17	none [d,e]
$\frac{7}{2} \to \frac{5}{2}$	1.12 8	0.48 14	$0.82 \leqq \delta \leqq 1.7$
$\frac{9}{2} \to \frac{5}{2}$	1.10 8	0.44 13	none [d,e]
879.6 (18 → 6)			
$\frac{3}{2} \to \frac{7}{2}$	−0.62 5	+0.23 8 [b]	none [d,e]
$\frac{5}{2} \to \frac{7}{2}$	−0.52 4	+0.30 11	none [e]
$\frac{7}{2} \to \frac{7}{2}$	−0.50 4	+0.22 8	none [e]
$\frac{9}{2} \to \frac{7}{2}$	−0.49 4	+0.23 8	−0.64±0.06
$\frac{11}{2} \to \frac{7}{2}$	−0.48 4	+0.22 8	none [e]
1409.6 (21 → 3)			
$\frac{3}{2} \to \frac{7}{2}$	0.79 11	0.01 12 [b]	none [d]
$\frac{5}{2} \to \frac{7}{2}$	0.66 9	0.02 16	−0.42 10
$\frac{7}{2} \to \frac{7}{2}$	0.63 9	0.01 13	none [d,e]
$\frac{9}{2} \to \frac{7}{2}$	0.62 9	0.01 12	0.18 5
$\frac{11}{2} \to \frac{7}{2}$	0.61 9	0.01 12	none [d,e]

[a] Based on $p(M = \frac{3}{2})/p(M = \frac{1}{2}) = 0.08$.
[b] The measured A_4 value is listed since the theoretical $R_4(J_1J_2\delta)$ for this spin sequence is zero.
[c] Fitted with A_4 set equal to zero, since other evidence established this level as $\frac{3}{2}$.
[d] No solution due to the $R_2(J_1J_2\delta)$ value.
[e] No solution due to the $R_4(J_1J_2\delta)$ value.
[f] Not given because this spin sequence is excluded on the basis of other evidence as discussed in the text.

TABLE 5

Summary of the quadrupole mixing for some transitions in ^{61}Cu

Transition (keV) (level sequence) $(J_1 \to J_2)$	% quadrupole content $Q = 100\delta^2/(1+\delta^2)$		
	this work [a]	Heusch *et al.* [3]	Adopted value [b]
970.3 (2 → 0)			
$(\frac{5}{2} \to \frac{3}{2})$	8.3 ± 2.0	12.6 ± 1.8	10.6 ± 1.5
		10.9 ± 1.8 [c]	
340.0 (3 → 2)			
$(\frac{7}{2} \to \frac{5}{2})$	0.0 ± 0.1	0	pure M1
919.2 (4 → 1)			
$(\frac{5}{2} \to \frac{1}{2})$	100	pure E2	pure E2
1394.6 (4 → 0)			
$(\frac{5}{2} \to \frac{3}{2})$	$0.04 \leqq Q \leqq 0.63$		
	or 89 ± 3	93 ± 1	92 ± 2
690.3 (5 → 2)			
$(\frac{3}{2} \to \frac{5}{2})$	$2.5 \leqq Q \leqq 16.2$	$0 \leqq Q \leqq 4.2$	3 ± 1
	or $\geqq 96$	or 91^{+4}_{-1}	or 93 ± 3
1185.3 (5 → 1)			
$(\frac{3}{2} \to \frac{1}{2})$		$6.3 \leqq Q \leqq 50$	$6.3 \leqq Q \leqq 50$
1660.4 (5 → 0)			
$(\frac{3}{2} \to \frac{3}{2})$	$9.8 \leqq Q \leqq 71$	$7.8 \leqq Q \leqq 74$	$9.8 \leqq Q \leqq 71$
421.7 (6 → 3)			
$(\frac{7}{2} \to \frac{7}{2})$	$5.4^{+7.8}_{-3.4}$	$3.8^{+4.0}_{-2.1}$	5^{+4}_{-3}
762.0 (6 → 2)			
$(\frac{7}{2} \to \frac{5}{2})$	17 ± 5	12^{+8}_{-5}	14 ± 3
593.5 (7 → 3)			
$(\frac{5}{2} \to \frac{7}{2})$	$0.2^{+0.4}_{-0.2}$		$0.2^{+0.4}_{-0.2}$
934.3 (7 → 2)			
$(\frac{5}{2} \to \frac{5}{2})$	$1.9^{+1.2}_{-0.9}$		$1.9^{+1.2}_{-0.9}$
1457.8 (8 → 1)			
$(\frac{3}{2} \to \frac{1}{2})$		3.8 ± 2.9 or 90^{+4}_{-7}	4 ± 3 or 90^{+4}_{-7}
1932.5 (8 → 0)			
$(\frac{3}{2} \to \frac{3}{2})$		$0.6 \leqq Q \leqq 15$	$0.6 \leqq Q \leqq 15$
		or $59 \leqq Q \leqq 86$	or $59 \leqq Q \leqq 86$
209.7 (9 → 6)			
$(\frac{7}{2} \to \frac{7}{2})$	$2.2^{+2.8}_{-1.7}$		$0.5 \leqq Q \leqq 5.0$
631.8 (9 → 3)			
$(\frac{7}{2} \to \frac{7}{2})$	$6.3^{+3.0}_{-2.5}$		$6.3^{+3.0}_{-2.5}$
	or $37^{+\ 9}_{-11}$		or 37 ± 10
352.1 (12 → 9)			

TABLE 5 (continued)

Transition (keV) (level sequence) ($J_1 = J_2$)	% quadrupole content $Q = 100\delta^2/(1+\delta^2)$		
	this work [a])	Heusch *et al.* [3])	Adopted value [b])
($\frac{9}{2} \rightarrow \frac{7}{2}$)	$10.9^{+2.9}_{-2.6}$		11 ± 3
562.5 (12 → 6)			
($\frac{9}{2} \rightarrow \frac{5}{2}$)	$23.9^{+7.1}_{-5.4}$		24^{+7}_{-5}
985.6 (12 → 3)			
($\frac{9}{2} \rightarrow \frac{7}{2}$)	$1.7^{+1.4}_{-1.1}$		$1.7^{+1.4}_{-1.1}$
1428.9 (15 → 2)			
($\frac{7}{2} \rightarrow \frac{5}{2}$)	$40 \leqq Q \leqq 74$		$40 \leqq Q \leqq 74$
879.6 (18 → 6)			
($\frac{9}{2} \rightarrow \frac{7}{2}$)	29 ± 4		29 ± 4
1409.6 (21 → 3)			
($\frac{9}{2} \rightarrow \frac{7}{2}$)	$3.1^{+1.9}_{-1.4}$		$3.1^{+1.9}_{-1.4}$

[a]) Here the quadrupole content is compared.
[b]) Weighted average value.
[c]) From ref. [15]).

defined and tabulated by Rose and Brink [4]). The coefficients Q_k are the angular correlation attenuation factors due to the finite solid angle of the Ge(Li) detector [12, 13]). Interpolated values from ref. [13]) were used in the analysis of these experiments. Under the conditions of the present experiments the population parameters $p(M_1)$ of the magnetic substates satisfy $\sum_{M_1} p(M_1) = 1$ and $p(-M_1) = p(M_1)$. Ideally, for a point proton detector at 180°, only $|M_1| = \frac{1}{2}$ substates contribute; however, in the present experiments substates other than $|M_1| = \frac{1}{2}$ may contribute due to the finite solid angle of the annular detector. Contributions from $|M_1| > \frac{1}{2}$ attenuate the correlation. As it is seen in the discussion below, the 919.2 keV transition between the ($\frac{5}{2}^-$) 1394.6 and ($\frac{1}{2}^-$) 475.0 keV levels is E2 in character. Since E2 transitions are not expected to mix with M3 multipoles one can use the correlation of this γ-ray to estimate the degree of alignment achieved in this reaction. This transition was too weak to give a reliable correlation in the coincidence experiments. From the singles correlation, however, it was possible to obtain the correlation shown in fig. 8d for this transition. Using the value $A_2(\text{exp}) = 0.53 \pm 0.05$ obtained from this correlation and assuming $p(\frac{5}{2}) = 0$ we calculate an upper limit for the ratio $p(\frac{3}{2})/p(\frac{1}{2})$ of $0.10 \pm^{0.16}_{0.10}$. We note that this alignment was obtained in the reaction without the coincidence restriction and therefore with the protons emitted in all directions. Furthermore, a number of γ-rays are known to populate the 1394.6 keV level and these would tend to increase the population of the $|M_1| = \frac{3}{2}$ and conceivably the $\frac{5}{2}$ substates. Both these effects indicate that the above ratio is indeed an upper limit. Since the coincidence pγ correlations were

found considerably more pronounced than the singles correlations and since most of the states investigated can decay by E2 and/or M1 transitions, it was safely assumed in the analysis of the data, that only the two lowest $|M_1|$ substates contributed with a ratio of $p(\frac{3}{2})/p(\frac{1}{2}) \leqq 0.08$ and that the states involved have $\tau \leqq 10$ ps which allowed the neglect of hyperfine perturbations. The analysis of the present results was made with $p(\frac{3}{2})/p(\frac{1}{2})$ equal to 0 and 0.08. The effect of this uncertainty on the δ-values for most of the cases was smaller than the quoted errors in table 4 where the results only for $p(\frac{3}{2})/p(\frac{1}{2})$ equal to 0.08 are presented. The first column of table 4 gives the transition energy, the level numbers characterizing the transition in the numbering of table 3, and the $J_1 \rightarrow J_2$ sequence considered. Columns 2 and 3 list the experimental values for $R_2(J_1 J_2 \delta)$ and $R_4(J_1 J_2 \delta)$ obtained by least-squares fits of eq. (2) to the data. The $R_k(J_1 J_2 \delta)$ values represent the quantity in curly brackets in eq. (2). The last column gives the mixing ratio δ for those $J_1 \rightarrow J_2$ sequences for which a solution within two standard deviations exists. Solutions are obtained when the points defined by experimental values of $R_2(J_1 J_2 \delta)$ and $R_4(J_1 J_2 \delta)$ are compared with the ellipses that result when the theoretical $R_2(J_1 J_2 \delta)$ is plotted versus $R_4(J_1 J_2 \delta)$ for all the δ-values and for each $J_1 \rightarrow J_2$ sequence.

In general the J^π assignments and the multipole mixing ratios δ from this work are in good agreement with the work of Heusch *et al.* [3]). In table 5 we summarize the percent quadrupole content $Q = [100\delta^2/(1+\delta^2)]$ from the δ-values of table 4 and from ref. [3]). The last column gives the adopted value for Q calculated as a weighted average of the individual values or as the overlapping values when a range of values is given.

4. Assignment of J^π values and discussion

On the basis of the evidence obtained in this work a detailed scheme for the decay of 50 levels in ^{61}Cu was constructed and it is shown in two portions in figs. 11 and 12. The energies of the γ-transitions are given in keV and in parentheses are given the branching fractions for the decay of each level. Arguments for the construction of the decay scheme and for the assignment of J^π values are summarized below.

The ground state. The ground state of ^{61}Cu is well established [1, 2]) as $\frac{3}{2}^-$.

The 475.0 *and* 2088.8 keV *levels.* These two levels are well established from the decay [2]) of ^{61}Zn. An $l_p = 1$ transfer has been assigned from the ^{60}Ni(^{3}He, d) work [ref. [14])] for the 475.0 keV level. These two levels are populated by allowed β^+ decay from the $\frac{3}{2}^-$ ^{61}Zn [log ft values 5.9 and 6.1, respectively [2])]. The singles angular distributions for the 475.0 and 2088.9 keV transitions were observed to be isotropic. This information limits the J^π for both these levels to $\frac{1}{2}^-$.

The 970.3 keV *level.* This level was observed in this work to decay to the ground and to the 475.0 keV levels. An $l_p = 3$ transfer in the ^{60}Ni(^{3}He, d) reaction [14]) limits the J^π value to $\frac{5}{2}^-$ or $\frac{7}{2}^-$. The pγ coincidence correlation (table 4) for the 970.3 keV

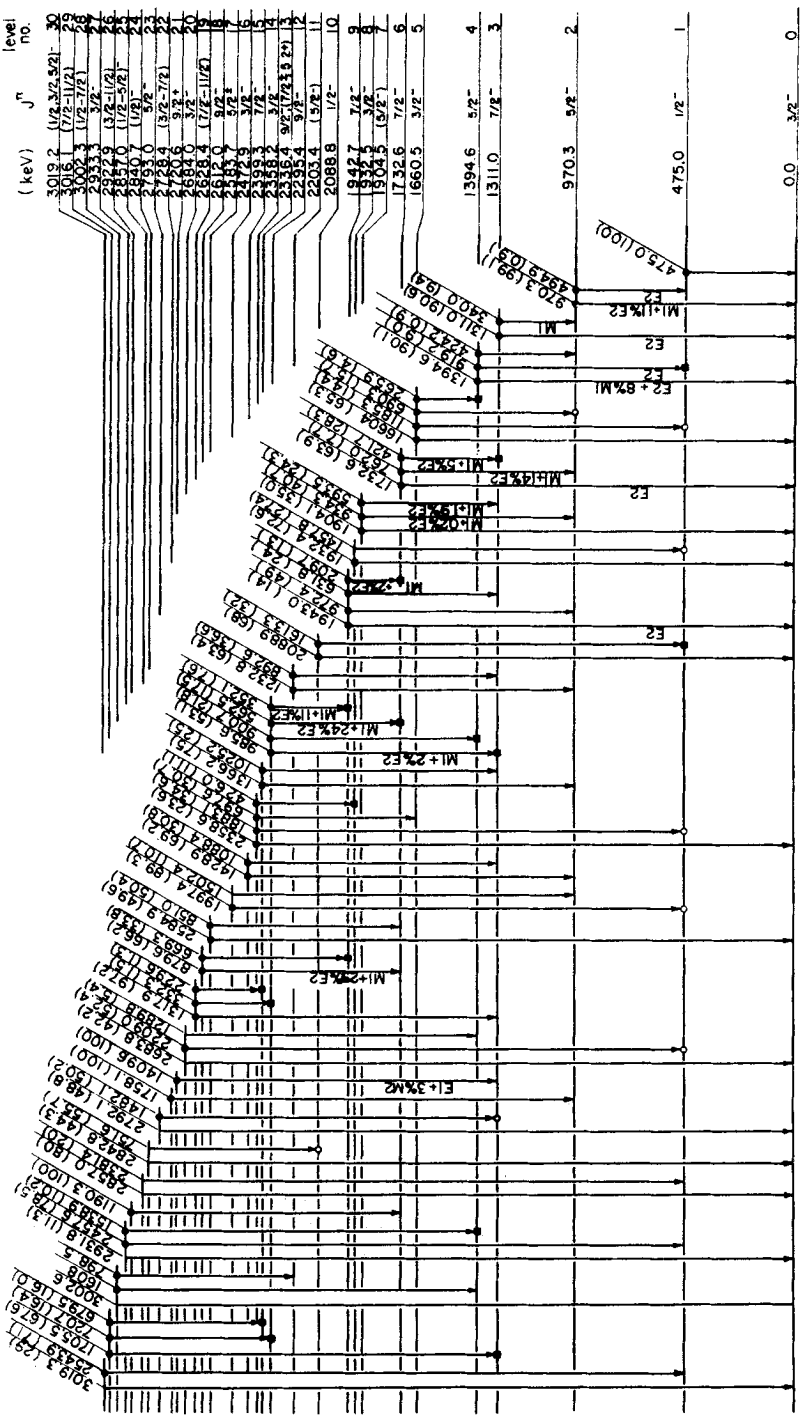

Fig. 11. Proposed scheme for the decay of levels in ^{61}Cu following excitation via the ^{58}Ni(^{4}He, pγ) reaction. Only the first 30 levels are included in this scheme. The energies are given in keV and the numbers in parentheses are the branching fractions for γ-decay.

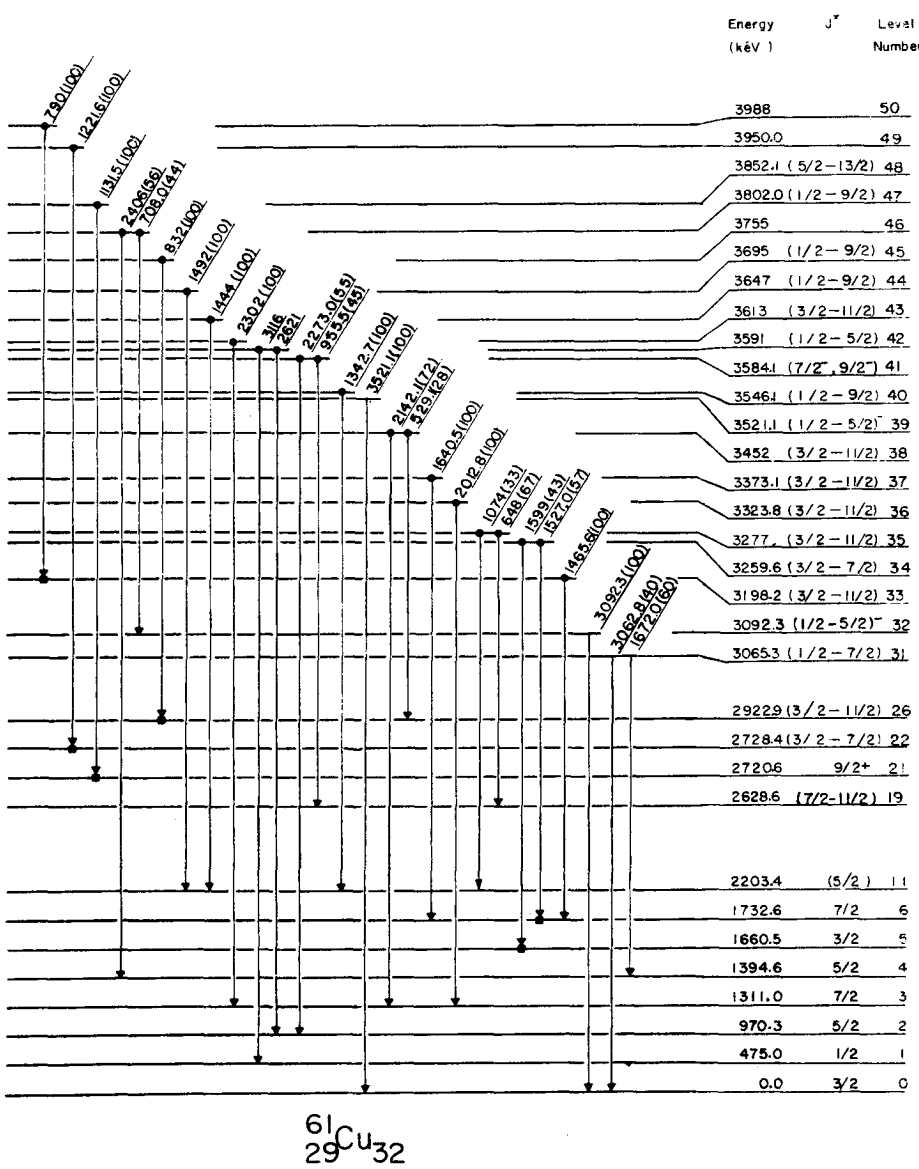

Fig. 12. Proposed scheme for the decay of levels in ^{61}Cu following excitation via the ^{58}Ni(^{4}He, pγ) reaction. Only levels no. 31 through 50 are shown together with those below no. 31 which are populated in their decay. The energies are given in keV and the numbers in parentheses are the branching fractions for γ-decay.

transition is consistent with only a $\frac{5}{2} \rightarrow \frac{3}{2}$ sequence. The 970.3 keV transition is found to be M1 in character with (10.6 ± 1.5) % E2 admixture (table 5).

The 1311.0 keV *level.* This level decays to the ground and the 970.3 keV levels. An $l_p = 3$ transfer in the ^{60}Ni(^{3}He, d) reaction [14]) limits J^π to $\frac{5}{2}^-$ or $\frac{7}{2}^-$ for this level. The pγ angular correlation for the 340.0 keV transition, from this work, is consistent with a $\frac{3}{2} \rightarrow \frac{5}{2}$ or $\frac{7}{2} \rightarrow \frac{5}{2}$ sequence (table 4). This level is not populated by β^+ decay of ^{61}Zn[log $ft > 7.9$, see ref. [2])] indicating a forbidden transition. The level at 2720.6 keV is shown below to be $\frac{9}{2}^+$ and it decays to the 1311.0 keV level by a 1409.6 keV transition. This 1409.6 keV transition has a pγ correlation (table 4) consistent only with a $\frac{9}{2} \rightarrow \frac{7}{2}$ and not with a $\frac{9}{2} \rightarrow \frac{5}{2}$ sequence.

The above information limits the J^π value for the 1311.0 keV level to $\frac{7}{2}^-$. The singles angular correlation for the 1311.0 keV transition peaks at 0° and this is consistent with a $\frac{7}{2}^- \rightarrow \frac{3}{2}^-$ E2 sequence.

The 340.0 keV transition is within experimental error pure M1 in character.

The 1394.6 keV *level.* This level decays to the ground, 475.0 and 970.3 keV levels. The pγ coincidence correlation of the 1394.6 keV transition is only consistent with a $\frac{5}{2} \rightarrow \frac{3}{2}$ sequence. This 1394.6 keV level was assigned an $l_p = (3)$ transfer [14]) from the ^{60}Ni(^{3}He, d) reaction which limits the possible J^π values to $\frac{5}{2}^-$. This transition appears to be almost pure E2 [see table 5 and ref. [3])]. The quadrupole content consistent with the pγ correlations is (92 ± 2) % E2.

The 1660.5 keV *level.* The decay of this level is well established [2]). The pγ coincidence correlations for the 690.3 and 1660.4 keV transitions from this level were measured (table 4). The correlation of the 690.3 keV transition is consistent only with a $\frac{3}{2} \rightarrow \frac{5}{2}$ or $\frac{7}{2} \rightarrow \frac{5}{2}$ sequence. The observed strong decay to the $\frac{1}{2}^-$ 475.0 keV level eliminates the $\frac{7}{2} \rightarrow \frac{5}{2}$ possibility. The pγ correlation for the 1660.5 keV transition is consistent only with the $\frac{3}{2} \rightarrow \frac{3}{2}$ and $\frac{5}{2} \rightarrow \frac{3}{2}$ sequences and definitely excludes the $\frac{7}{2} \rightarrow \frac{3}{2}$ possibility (table 4). The pγ correlation for the 1185.3 keV transition was examined and although it was of poor statistical quality to give good values for A_2 and A_4, it definitely showed a maximum at 90°. Since for aligned states all E2 transitions yield always a maximum at 0°, a sequence of $\frac{5}{2} \rightarrow \frac{1}{2}$ for this transition must be eliminated. This limits the assignment for this 1660.4 keV level to $\frac{3}{2}^-$.

The correlation of the 690.3 keV transition is consistent with either an M1 character with (3 ± 1) % E2 admixture or E2 with (7 ± 3) % M1 admixture (table 5). For the 1185.3 and 1660.4 keV transitions only the broad limits of table 5 for the quadrupole admixture can be placed from the existing evidence.

The 1732.6 keV *level.* This level decays to the $(\frac{3}{2}^-)$ ground, $(\frac{5}{2}^-)$ 970.3 and $(\frac{7}{2}^-)$ 1311.0 keV states. This level is not populated in the β-decay [2]) in ^{61}Zn nor in the ^{60}Ni(^{3}He, d) reaction [14]). The pγ correlation for the 762.0 keV transition to the $(\frac{5}{2}^-)$ 970.3 keV level is consistent with a $\frac{5}{2} \rightarrow \frac{5}{2}$ or $\frac{7}{2} \rightarrow \frac{5}{2}$ sequence. The pγ correlation for the 721.7 keV transition, however, is consistent only with a $\frac{7}{2} \rightarrow \frac{7}{2}$ sequence. This limits the J-value for this level to $\frac{7}{2}$. The parity of this level must be negative, since a positive parity would require the strong 1732.6 keV transition to the ground state to be M2 in character and this is very unlikely.

The 421.7 and 762.0 keV transitions are M1 character with (5^{+4}_{-3}) % and (14 ± 3) % E2 admixtures, respectively (table 5).

The 1904.5 keV *level.* This level is not populated in the (^{3}He, d) reaction [14]) and is only weakly populated in the β-decay [2]) of ^{61}Zn. In this work this level was observed to decay to the ground, the 970.3 and 1311.0 keV levels. The coincidence pγ correlation for the 593.5 keV transition to the 1311.0 keV definitely eliminates the $\frac{3}{2} \rightarrow \frac{7}{2}$ and $\frac{1}{2} \rightarrow \frac{7}{2}$ sequences (table 4) and is consistent with a $\frac{5}{2} \rightarrow \frac{7}{2}$, $\frac{7}{2} \rightarrow \frac{7}{2}$ or $\frac{9}{2} \rightarrow \frac{7}{2}$ sequence. On the other hand the pγ correlation for the 934.3 keV transition to the 970.3 keV level definitely eliminates the $\frac{9}{2} \rightarrow \frac{5}{2}$ sequence and is consistent with the $\frac{5}{2} \rightarrow \frac{5}{2}$ and $\frac{7}{2} \rightarrow \frac{5}{2}$ sequences (table 4). The singles correlation for the 1904.1 keV transition to the $\frac{3}{2}^-$ ground state was observed to be strongly peaked at 0° and this is not inconsistent with $\frac{7}{2}$ or $\frac{5}{2}$ for this level. The fact that this level is seen in the ^{61}Zn decay can be further used [2]) to limit J^π to $\frac{5}{2}^-$.

If the J^π value were indeed $\frac{5}{2}^-$ then the 593.5 and 934.3 keV transitions would be M1 with $(0.3^{+0.4}_{-0.2})$ and $(1.9^{+1.2}_{-0.9})$ % E2 character, respectively (table 5).

The 1932.5 keV *level.* This level was also observed in the β-decay of the $(\frac{3}{2}^-)$ ^{61}Zn by an allowed transition [2]) ($\log ft = 6.1$). This level should be identified with the level at 1940 keV from the (^{3}He, d) reaction which was reported by Pullen and Rosner [ref. [14])] to have $l_p = 1$. This limits J^π for this level to $\frac{1}{2}^-$ or $\frac{3}{2}^-$. The pγ angular distribution was seen to have definitely a maximum at 90° and this eliminates the $\frac{1}{2}^-$ value as a possibility. Thus, a $\frac{3}{2}^-$ assignment is made for this level.

The 1942.7 keV *level.* This level was not observed [2]) in the β-decay of ^{61}Zn and it does not appear to be populated in the (^{3}He, d) reaction [14]). In this work four γ-rays at 209.7, 631.8, 972.4 and 1943.0 keV have been assigned to de-excite this level. The 970.3, 972.4 keV doublet was identified from an upward shift of 1 keV in the coincidence spectrum of fig. 6b. Both the pγ coincidence correlations for the 209.7 and 631.8 keV transitions to the $(\frac{7}{2}^-)$ levels at 1732.6 and 1311.0 keV are consistent only with a $\frac{7}{2} \rightarrow \frac{7}{2}$ sequence (table 4). This information limits the J-value for this level to $\frac{7}{2}$. The parity of this level must be negative, since a positive parity would require the strong branch to the $\frac{3}{2}^-$ ground state to be an M2 transition, which is very unlikely. Therefore, the 209.7 keV transition is M1 in character with $(2.2^{+2.8}_{-1.7})$ % E2 admixture, while the 631.8 keV transition is M1 in character with $(3.6^{+3.0}_{-2.5})$ or (37 ± 10) % E2 admixture (table 5).

The 2203.4 keV *level.* This level is populated weakly in the ^{61}Zn β-decay [2]) ($\log ft = 6.8$). It should be identified with the level at 2216 keV reported in the (^{3}He, d) reaction study [14]) to have $l_p = 3$. This indicates a $J^\pi = \frac{5}{2}^-$ or $\frac{7}{2}^-$ assignment. The fact that this level was observed in the ^{61}Zn decay helps eliminate the $\frac{7}{2}^-$ value as a possibility, since this would require a second-forbidden β^+ decay which should not have been observed [2]). This information limits the J^π value for this level to $\frac{5}{2}^-$.

The 2295.4 keV *level.* This level was established in this work to de-excite via the 352.1, 562.5, 900.7 and 985.6 keV transitions to the $(\frac{7}{2}^-)$1442.7, $(\frac{7}{2}^-)$1732.6, $(\frac{5}{2}^-)$ 1394.6 and $(\frac{7}{2}^-)$1311.0 keV levels. This level is not observed in the ^{61}Zn decay. In this work the pγ coincidence correlations for the 352.1 and 985.6 keV transitions were measured and both were found consistent with a $\frac{5}{2} \rightarrow \frac{7}{2}$ or $\frac{9}{2} \rightarrow \frac{7}{2}$ sequence. Furthermore, the pγ correlation for the 562.5 keV transition was measured and it was found consistent only with a $\frac{9}{2} \rightarrow \frac{7}{2}$ sequence. This evidence establishes the J-value for this level as $\frac{9}{2}$. The large quadrupole admixtures for both the 352.1 and 562.5 keV transitions exclude a positive-parity assignment for this level. The 352.1, 562.5 and 985.6 keV transitions are, therefore, M1 in character with (11 ± 3), (24^{+7}_{-5}) and $(1.7^{+1.4}_{-1.1})$ % E2 admixtures, respectively (table 5).

The 2336.4 keV *level.* This level was established in this work to decay only to the $(\frac{5}{2}^-)$970.3 and $(\frac{7}{2}^-)$1311.0 keV levels. This limits the possible J^π values to $\frac{3}{2}^-$, $\frac{5}{2}^\pm$, $\frac{7}{2}^\pm$ or $\frac{9}{2}^-$ for this level. The singles angular correlation for the 1025.2 keV γ-ray to the $(\frac{7}{2}^-)$1311.0 keV level has a strong maximum at 90° and this is sufficient to exclude the $\frac{3}{2}^-$ value, as this would require an E2 transition which for aligned nuclei has always a maximum at 0° to the beam direction. This level is not populated [2]) in the β-decay of ^{61}Zn and this indicates that a $\frac{5}{2}^-$ value is very unlikely. Furthermore, the lack of decay to the $(\frac{3}{2}^-)$ ground and $(\frac{1}{2}^-)$475.0 keV levels suggests a high J-value for this level. Although on shell-model considerations the positive-parity states should lie even higher in excitation we cannot with certainty exclude the possibility of $\frac{5}{2}^+$ or $\frac{7}{2}^+$ for this level. On the basis of the above evidence we favor a $\frac{9}{2}^-$ assignment for this level, although we cannot exclude the $\frac{5}{2}^+$ or $\frac{7}{2}^\pm$ as possibilities.

The 2358.2, 2472.9, 2684.0 *and* 2933.3 keV *levels.* These four levels have been observed [2]) in the β-decay of ^{61}Zn with logft values indicating allowed transitions. All these levels decay to the $(\frac{1}{2}^-)$475.0 keV level and none of the corresponding γ-rays had an isotropic singles angular distribution. This evidence limits the J^π value to $\frac{3}{2}^-$ or $\frac{5}{2}^-$ for these levels. The singles angular correlations of the γ-rays from the decay of each of these levels to the $(\frac{1}{2}^-)$475.0 keV state were observed to have a definite maximum at 90° and this excludes a $\frac{5}{2} \rightarrow \frac{1}{2}$ sequence for these transitions. The J^π value for these levels is therefore limited to $\frac{3}{2}^-$.

The 2399.3 keV *level.* This level is established to decay to the $(\frac{5}{2}^-)$970.3 and $(\frac{7}{2}^-)$ 1311.0 keV levels. This level was not seen in the ^{61}Zn β-decay. The pγ coincidence correlation for the 1428.9 keV transition to the $(\frac{5}{2}^-)$ 970.3 keV level is consistent only with the $\frac{7}{2} \rightarrow \frac{5}{2}$ sequence. This is further confirmed by the observed strong maximum at 90° of the singles correlation for the 1428.9 keV γ-ray which definitely excludes a $\frac{3}{2}$ or $\frac{9}{2}$ assignment. The 1428.9 keV transition was seen to have a large quadrupole content $40 \leqq Q \leqq 74$. The large observed quadrupole admixture for the 1428.9 keV transition can be used to eliminate the positive parity as a possible one for this level, since this would require a large M2 admixture in an E1 transition which is very unlikely. The above information, therefore, limits the J^π value for this level to $\frac{7}{2}^-$.

The 2583.7 keV *level.* This was not observed in the β-decay of ^{61}Zn but it was established in this work to decay to the ground state and the 1311.0 keV level. Since this level decays to $\frac{3}{2}^-$ and $\frac{7}{2}^-$ levels below, its J^π can be limited to $\frac{3}{2}^-$, $\frac{5}{2}^\pm$ or $\frac{7}{2}^-$. The singles angular correlation for the 2584.9 keV γ-ray has a definite maximum at 90° and this may be used to exclude a $\frac{7}{2} \rightarrow \frac{3}{2}$ sequence. Also, the singles correlation for the 851.0 keV γ-ray has a definite maximum at 90° and this eliminates the $\frac{3}{2} \rightarrow \frac{7}{2}$ sequence as a possibility for this transition. The present evidence limits J^π for this level to $\frac{5}{2}^\pm$.

The 2612.0 keV *level.* This level was established in this work to decay to the $(\frac{7}{2}^-)$ 1732.6 and $(\frac{7}{2}^-)$ 1942.7 keV levels, via 879.6 and 669.3 keV transitions, respectively. The pγ coincidence correlation for the 879.6 keV transitions was measured and found consistent only with a $\frac{9}{2} \rightarrow \frac{7}{2}$ sequence (table 4). A positive parity for this level would require the 879.6 keV transition to be E1 with an M2 admixture of (29 ± 4) % which is too high to be likely. We therefore limit J^π for this level to $\frac{9}{2}^-$.

The 2628.4 keV *level.* The 2628.4 keV level was established to decay to the $(\frac{7}{2}^-)$ 1311.0, $(\frac{9}{2}^-)$ 2295.4 and $(\frac{9}{2}^-)$ 2336.4 keV levels. The singles angular distribution for the 332.3 keV transition to the 2295.4 keV level has a definite maximum at 90° and this restrict J^π for the 2628.4 keV level to $\frac{7}{2}^-$, $\frac{9}{2}^\pm$, or $\frac{11}{2}^-$, since the 2295.4 keV level is $\frac{9}{2}^-$. The lack of decay to any of low spin levels below, however, tends to favor the higher J^π values for this level.

The 2720.6 keV *level.* This level was observed in this work to decay only via a 1409.6 keV transition to the $(\frac{7}{2}^-)$ 1311.0 keV level. A level at 2711 keV with an $l_p = 4$ was reported [14]) to be populated in the (^{3}He, d) reaction and it should be identified with the 2720.6 keV level. The $l_p = 4$ assignment restricts J^π to $\frac{7}{2}^+$ or $\frac{9}{2}^+$ for this level. The pγ coincidence correlation for the 1409.6 keV transition definitely excludes the $\frac{3}{2} \rightarrow \frac{7}{2}$, $\frac{7}{2} \rightarrow \frac{7}{2}$ or $\frac{11}{2} \rightarrow \frac{7}{2}$ sequences and it is consistent only with a $\frac{5}{2} \rightarrow \frac{7}{2}$ or $\frac{9}{2} \rightarrow \frac{7}{2}$ sequence. The above evidence is sufficient to limit J^π to $\frac{9}{2}^+$ for this level. The 1409.6 keV transition is then E1 in character with $(3.1 \pm^{1.9}_{1.4})$ % M2 admixture which is not unlikely in view of the large error associated with the multiple mixing ratio.

The 2728.4 keV *level.* This level was established in this work to decay only to the $(\frac{5}{2}^-)$ 970.3 keV level via a 1758.1 keV transition. Both the singles and pγ correlations for the 1758.1 keV γ-ray have a definite maximum at 90°. This evidence limits J^π for this level to $\frac{3}{2}$, $\frac{5}{2}$ or $\frac{7}{2}$.

The 2793.0 keV *level.* This level is populated in the β-decay of ^{61}Zn by an allowed transition [2]) ($\log ft = 5.1$), and this limits J^π to $\frac{1}{2}^-$, $\frac{3}{2}^-$ or $\frac{5}{2}^-$ for this level. Since this level was observed to decay to levels with J^π of $\frac{7}{2}^-$ we may exclude the $\frac{1}{2}^-$ possibility. The 1482.1 keV transition to the $(\frac{7}{2}^-)$ 1311.0 keV level has a singles angular distribution with a maximum at 90° and this excludes a $\frac{3}{2} \rightarrow \frac{7}{2}$ sequence for this transition. This evidence limits J^π for this level to $\frac{5}{2}^-$.

The 2840.7 keV *level.* This level is populated by an allowed [2]) β-decay from ^{61}Zn ($\log ft = 5.5$) and this limits J^π to $\frac{1}{2}^-$, $\frac{3}{2}^-$ or $\frac{5}{2}^-$ for this level. A level at 2846 was

reported from the (^{3}He, d) reaction [14]) to have an $l_p = 1$ transfer and this restricts J^π to $\frac{1}{2}^-$ or $\frac{3}{2}^-$ for this level with a probable [14]) value of $\frac{1}{2}^-$.

The 2857.0, 3019.2, 3092.3 *and* 3521.1 keV *levels.* These levels have been also observed to be populated by allowed β-decay from ^{61}Zn(log ft = 5.5, 5.6, 5.8 and 5.2, respectively) and on this basis they have been assigned [2]) as $\frac{1}{2}^-$, $\frac{3}{2}^-$ or $\frac{5}{2}^-$.

The 2922.9, 3198.2, 3323.8, 3373.1 *and* 3613 keV *levels.* These levels were established in this work and from pγ coincidence information were shown to decay only to the levels at 1732.6, 1732.6, 1311.0, 1732.6 and 1311.0 keV, respectively, all of which are $\frac{7}{2}^-$. This limited information restricts J^π for these levels only to $\frac{3}{2}^-$, $\frac{5}{2}^-$, $\frac{7}{2}^\pm$, $\frac{9}{2}^+$ or $\frac{11}{2}^-$.

The 3002.6 *and* 3065.3 keV *levels.* These levels were established in this work and from pγ coincidence information were shown to populate only levels with J^π of $\frac{3}{2}^-$ and $\frac{5}{2}^-$ below (see figs. 11 and 12). This information limits J^π for these levels to $\frac{1}{2}^-$, $\frac{3}{2}^\pm$, $\frac{5}{2}^\pm$ or $\frac{7}{2}^-$.

The 3016.4 keV *level.* This level is established to decay only to the $(\frac{7}{2}^-)$1311.0, $(\frac{9}{2}^-)$ 2295.4 and $(\frac{9}{2}^-)$ 2336.4 keV levels. This evidence together with the lack of decay to levels with $J^\pi \leqq \frac{5}{2}$ suggests a high J^π value of $\frac{7}{2}^-$, $\frac{9}{2}^\pm$ or $\frac{11}{2}^-$ for this level.

The 3277 *and* 3452 keV *levels.* These levels have been shown to decay to the $(\frac{7}{2}^-)$ levels at 2399.3 and 1311.0 keV, respectively, and to the $(\frac{7}{2}^-\frac{11}{2})$ 2628.4 and $(\frac{3}{2}^-\frac{11}{2})$ 2922.9 keV levels below, respectively. This limited information restricts J^π for these levels to $\frac{3}{2}^-$, $\frac{5}{2}^\pm$, $\frac{7}{2}^\pm$, $\frac{9}{2}^\pm$ or $\frac{11}{2}^-$.

The 3456.1, 3647 *and* 3695 keV *levels.* These levels were established in this work to decay only to the $(\frac{5}{2}^-)$ level at 2203.4 keV. This limited information permits one to limit J^π for these levels to $\frac{1}{2}^-$, $\frac{3}{2}^\pm$, $\frac{5}{2}^\pm$, $\frac{7}{2}^\pm$ or $\frac{9}{2}^-$.

The 3584.1 keV *level.* This level was established from pγ coincidence information to decay to the $(\frac{5}{2}^-)$ 970.3 and $(\frac{11}{2}^-, \frac{9}{2}^-)$ 2628.6 keV levels. This evidence limits J^π for this level to $\frac{7}{2}^-$ or $\frac{9}{2}^-$.

The 3591 keV *level.* This level was shown from pγ coincidence information to decay to the $(\frac{1}{2}^-)$ 475.0 and $(\frac{5}{2}^-)$ 970.3 keV levels. This limited evidence restricts J^π for this level to $\frac{1}{2}^-$, $\frac{3}{2}^\pm$ or $\frac{5}{2}^-$.

The 3802.0 keV *level.* This level was shown to decay to the $(\frac{5}{2}^-)$ level at 1394.6 keV and to the $(\frac{5}{2}^-, \frac{3}{2}^-)$ level at 3094.0 keV. This information limits J^π for the 3802.0 keV level to $\frac{1}{2}^\pm$, $\frac{3}{2}^\pm$, $\frac{5}{2}^\pm$, $\frac{7}{2}^\pm$ or $\frac{9}{2}^-$.

The 3852.1 keV *level.* This level was established to decay only to the $\frac{9}{2}^+$ level at 2720.6 keV and this limits J^π for this level to $\frac{5}{2}^+$, $\frac{7}{2}^\pm$, $\frac{9}{2}^\pm$, $\frac{11}{2}^\pm$ or $\frac{13}{2}^+$.

The 3755, 3950.0 *and* 3988 keV *levels.* These levels were established in this work to decay to the 2922.9, 2738.4 and 3198.2 keV levels, respectively. The large range of

possible J^π values for the latter mentioned levels does not permit any assignment of J^π values to the 3755, 3950.0 and 3988 keV levels at the present time.

We wish to express our thanks to Mr. John Hood and the personnel of the Washington University cyclotron for the continued cooperation during the course of these experiments. The cooperation of the staff of the Washington University computing facilities is appreciated. We also wish to thank Dr. A. Friedman for his assistance in the experiments at the Argonne National Laboratory.

References

1) E. J. Hoffman and D. G. Sarantites, Phys. Rev. **177** (1969) 1647
2) E. J. Hoffman and D. G. Sarantites, Nucl. Phys. **A157** (1970) 584
3) B. Heusch, B. Čujec, R. Dayras, J. N. Mo et I. M. Szöghy, Nucl. Phys. **A169** (1971) 145
4) D. G. Sarantites and W. G. Winn, Nucl. Phys. **A155** (1970) 257
5) J. W. Luetzelschwab, Ph.D. thesis, Washington University (1968) unpublished
6) M. E. Phelps, D. G. Sarantites and W. G. Winn, Nucl. Phys. **A149** (1970) 647
7) J. E. Spencer and H. A. Enge, Nucl. Instr. **49** (1967) 181
8) J. R. Erskine and R. H. Vonderohe, Argonne Physics Division, Report PHYS-1969F, Dec. 1969
9) J. C. Ritter and R. E. Larson, Nucl. Phys. **A127** (1969) 399
10) D. M. Van Patter, R. N. Horoshko and H. L. Scott, Nucl. Phys. **A137** (1969) 353
11) H. J. Rose and D. M. Brink, Rev. Mod. Phys. **39** (1967) 306
12) W. G. Winn and D. G. Sarantites, Nucl. Instr. **66** (1967), 61; **82** (1970) 230
13) D. C. Camp and A. V. Van Lehn, Nucl. Instr. **76** (1969) 192
14) D. J. Pullen and B. Rosner, Phys. Rev. **170** (1968) 1034
15) C. R. Gossett and L. S. August, Phys. Rev. **137** (1965) B381